Inorg. Chem. **2004**, *43*, 1137−1152

Bacterial Iron Transport: Coordination Properties of Azotobactin, the Highly Fluorescent Siderophore of *Azotobacter vinelandii*

Tania Palanché,[†] Sylvie Blanc,[†] Christophe Hennard,[‡] Mohamed A. Abdallah,*[,‡] and Anne-Marie Albrecht-Gary*[,†]

Laboratoire de Physico-Chimie Bioinorganique, CNRS UMR 7509, ECPM, 25, Rue Becquerel, 67200 Strasbourg, France, and Laboratoire de Chimie Microbienne, CNRS UPR 9050, Département des Récepteurs et Protéines Membranaires, Ecole Supérieure de Biotechnologie de Strasbourg, Boulevard Sébastien Brant, 67400 Illkirch, France

Received July 21, 2003

Azotobacter vinelandii, a nitrogen-fixing soil bacterium, secretes in iron deficiency azotobactin δ, a highly fluorescent pyoverdin-like chromopeptidic hexadentate siderophore. The chromophore, derived from 2,3-diamino-6,7 dihydroxyquinoline, is bound to a peptide chain of 10 amino acids: (L)-Asp-(D)-Ser-(L)-Hse-Gly-(D)-β-*threo*-HOAsp-(L)-Ser-(D)-Cit-(L)-Hse-(L)-Hse lactone-(D)-N$^{\delta}$-Acetyl, N$^{\delta}$-HOOrn. Azotobactin δ has three different iron(III) binding sites which are one hydroxamate group at the C-terminal end of the peptidic chain (N$^{\delta}$-Acetyl, N$^{\delta}$-HOOrn), one α-hydroxycarboxylic function in the middle of the chain (β-*threo*-hydroxyaspartic acid), and one catechol group on the chromophore. The coordination properties of its iron(III) and iron(II) complexes were measured by spectrophotometry, potentiometry, and voltammetry after the determination of the acid–base functions of the uncomplexed free siderophore. Strongly negatively charged ferric species were observed at neutral p[H]'s corresponding to a predominant absolute configuration Λ of the ferric complex in solution as deduced from CD measurements. The presence of an α-hydroxycarboxylic chelating group does not decrease the stability of the iron(III) complex when compared to the main trishydroxamate siderophores or to pyoverdins. The value of the redox potential of ferric azotobactin is highly consistent with a reductive step by physiological reductants for the iron release. Formation and dissociation kinetics of the azotobactin δ ferric complex point out that both ends of this long siderophore chain get coordinated to Fe(III) before the middle. The most striking result provided by fluorescence measurements is the lasting quenching of the fluorophore in the course of the protonation of the ferric azotobactin δ complex. Despite the release of the hydroxyacid and of the catechol, the fluorescence remains indeed quenched, when iron(III) is bound only to the hydroxamic acid, suggesting a folded conformation at this stage, around the metal ion, in contrast to the unfolded species observed for other siderophores such as ferrioxamine or pyoverdin PaA.

Introduction

Azotobacter vinelandii is a nitrogen-fixing bacterium that transforms atmospheric nitrogen into ammonia.[1,2] Only a relatively small number of microorganisms termed diazotrophs[3] are capable of carrying out this process, and all organisms depend directly or indirectly upon them for their supply of nitrogenated compounds used for the synthesis of nucleic acids. This biological reduction of atmospheric nitrogen into ammonia which is called nitrogen fixation is due to a multimeric enzyme called nitrogenase which catalyzes the conversion of molecular nitrogen N_2 into ammonia NH_3. The nitrogenases occur in *Rhizobia*, bacteria living symbiotically in some plants roots (beans, peas, alfalfa), or in free soil bacteria such as *Azotobacter, Klebsiella, Azospirillum, Azomonas*, etc., or in blue green algae (cyanobacteria). These enzymes possess two proteic compartments: one containing iron (Fe-protein) and the other either iron and molybdenum (MoFe-protein), or iron and

* Authors to whom correspondence should be addressed. E-mail: abdallah@esbs.u-strasbg.fr (M.A.A.); amalbre@chimie.u-strasbg.fr (A.-M.A.-G.).
[†] Laboratoire de Physico-Chimie Bioinorganique.
[‡] Laboratoire de Chimie Microbienne.

(1) Glick, B. R. *Can. J. Microbiol.* **1995**, *41*, 109−117.
(2) Page, W. J. In *Iron Chelation in Plants and Soil Microorganism*; Barton, L. L., Hemming, B. C., Eds.; Academic Press: San Diego, CA, 1993; pp 75−110.
(3) Kim, J.; Rees, D. C. *Biochemistry* **1994**, *33*, 389−397.

10.1021/ic034862n CCC: $27.50
Published on Web 12/31/2003

vanadium (V−Fe-protein). This underlines the particularly crucial role of iron for the survival of the bacterium for which nitrogen supply can be subject to iron uptake.

Under iron deficient conditions *Azotobacter vinelandii* (strain D) secretes high amounts of a fluorescent siderophore called azotobactin,[4] a chromopeptidic siderophore belonging to the class of pyoverdins, the peptidic siderophores of the fluorescent pseudomonads.[5] Pyoverdins are constituted of a fluorescent chromophore derived from 2,3-diamino-6,7-dihydroxyquinoline, bound via a carboxylic acid group to the N terminus of an oligopeptide of 6−12 amino acids of various chirality and composition with a linear,[6−14] partially cyclic,[15−19] or fully cyclic[20] backbone.

All of these siderophores, pyoverdins or pyoverdin-like siderophores, possess three iron(III) specific bidentate groups: the catechol group of the fluorophore, one hydroxamate group at the end of the peptidic chain, and either an additional hydroxamate group or a hydroxycarboxylic acid group in the middle of the chain. These bidentate groups firmly bind to iron(III) giving very stable octahedral complexes by means of six oxygen atoms.

Structure elucidation of azotobactin δ has shown that the three different iron(III) binding sites are one hydroxamate group at the C-terminal end of the peptidic chain (N^{δ}-acetyl, N^{δ}-HOOrn), one α-hydroxycarboxylic function in the middle of the chain (*β-threo*-hydroxyaspartic acid), and one catechol group on the fluorophore derived from 2,3-diamino-6,7 dihydroxyquinoline.[4] The latter is bound to a peptide chain of 10 amino acids: (L)-Asp-(D)-Ser-(L)-Hse-Gly-(D)-*β-threo*-HOAsp-(L)-Ser-(D)-Cit-(L)-Hse-(L)-Hse lactone-(D)-N^{δ}-acetyl, N^{δ}-HOOrn (Figure 1).[104] In solution, azotobactin D is in equilibrium with its lactone form azotobactin δ. Lactonization of the terminal homoserine did not show any effect on the ability of azotobactin δ to function as a siderophore.[21,22]

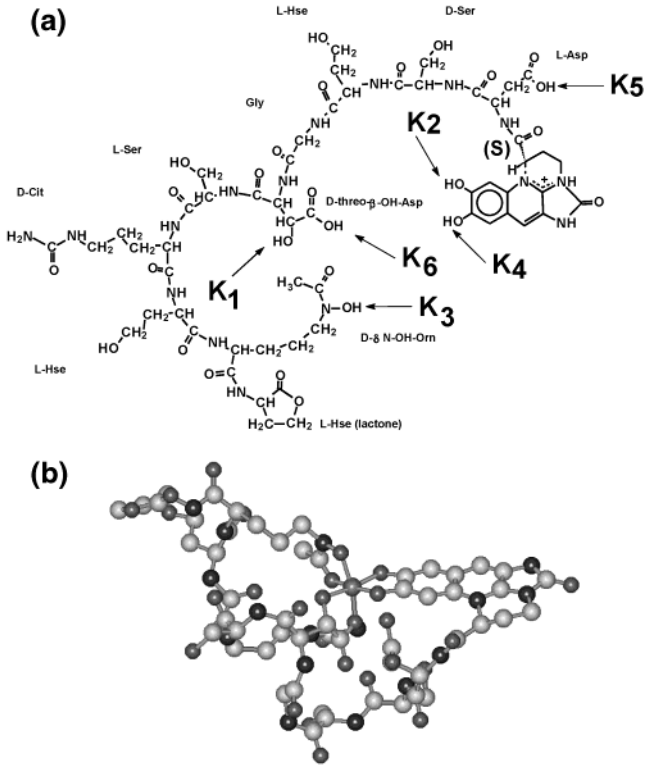

Figure 1. (a) Chemical structure of azotobactin δ. K_1−K_6: protonation constants. (b) Model of azotobactin δ Fe(III) complex.

We report here a physicochemical approach for the determination of the coordination properties of the iron(III) and iron(II) complexes of azotobactin δ using various spectrophotometric methods: absorption, fluorescence,[23] and circular dichroism, in order to fully characterize its ferric complexes present in equilibrium under various acidic conditions. The cyclic voltammetric data providing information about a possible physiological reduction process of ferric azotobactin δ and its efficiency in a release mechanism are also reported. For a better understanding of the iron uptake and release process,[24−26] respectively outside and inside the *Azotobacter vinelandii* cell, the kinetic data related to the formation and dissociation of ferric azotobactin δ are also presented. Both absorption and fluorescence detections were used in order to gain an insight into the structure of intermediate ferric species.

From this comprehensive study, it was possible to point out the thermodynamic, electrochemical, and kinetic contribution of the central α-hydroxycarboxylic moiety compared with the hydroxamate group present in pyoverdin PaA, the peptidic siderophore of *Pseudomonas aeruginosa*.[27] As α-hydroxycarboxylic acids are the most commonly occurring

(4) Demange, P.; Bateman, A.; Dell, A.; Abdallah, A. M. *Biochemistry* **1988**, *27*, 2745−2752.
(5) Pattus, F.; Abdallah, M. A. *J. Chin. Chem. Soc.* **2000**, *47*, 1−20.
(6) Teintze, M.; Hossain, M. B.; Barnes, C. L.; Leong, J.; van der Helm, D. *Biochemistry* **1981**, *20*, 6446−6457.
(7) Wendenbaum, S.; Demange, P.; Dell, A.; Meyer, J. M.; Abdallah, M. A. *Tetrahedron Lett.* **1983**, *24*, 4877−4880.
(8) Mohn, G.; Taraz, K.; Budzikiewicz, H. *Z. Naturforsch.* **1990**, *45b*, 1437−1450.
(9) Persmark, M.; Frejd, T.; Mattiason, B. *Biochemistry* **1990**, *29*, 7348−7356.
(10) Demange, P.; Bateman, A.; Mertz, C.; Dell, A.; Piémont, Y.; Abdallah, A. M. *Biochemistry* **1990**, *29*, 11041−11051.
(11) Linget, C.; Collinson, S. K.; Azadi, P.; Dell, A.; Page, W. J.; Abdallah, M. A. *Tetrahedron letters* **1992**, *33*, 1889−1892.
(12) Bernardini, J. J.; Linget-Morice, C.; Hoh, F.; Collinson, S. K.; Kyslik, P.; Page, W. J.; Dell, A.; Abdallah, M. A. *BioMetals* **1996**, *9*, 107−120.
(13) Milchalke, R.; Taraz, K.; Budzikiewicz, H. *Z. Naturforsch.* **1996**, *51c*, 772−780.
(14) Salah El Din, A. L. M.; Kyslik, P.; Stephan, D.; Abdallah, M. A. *Tetrahedron* **1997**, *53*, 12539−12552.
(15) Poppe, K.; Taraz, K.; Budzikiewicz, H. *Tetrahedron* **1987**, *43*, 2261−2272.
(16) Briskot, G.; Taraz, K.; Budzikiewicz, H. *Liebigs Ann. Chem.* **1989**, 375−384.
(17) Hohlneicher, U.; Hartmann, R.; Taraz, K.; Budzikiewicz, H. *Z. Naturforsch.* **1992**, *47b*, 1633−1638.
(18) Geisen, K.; Taraz, K.; Budzikiewicz, H. *Monatsh. Chem.* **1992**, *123*, 151−178.
(19) Hohlneicher, U.; Hartmann, R.; Taraz, K.; Budzikiewicz, H. *Z. Naturforsch.* **1995**, *50c*, 337−344.
(20) Yang, C. C.; Leong, J. *Biochemistry* **1984**, *23*, 3534−3540.
(21) Page, W. J.; Huyer, M. *J. Bacteriol.* **1984**, *158*, 496−502.
(22) Knosp, O.; Von Tigerstrom, M.; Page, W. J. *J. Bacteriol*. **1984**, *159*, 341−347.
(23) Palanché, T.; Marmolle, F.; Abdallah, M. A.; Shanzer, A.; Albrecht-Gary, A. M. *JBIC, J. Biol. Inorg. Chem.* **1999**, *4*, 188−198.
(24) Boukhalfa, A.; Brickman, T. J.; Armstrong, S. K.; Crumbliss, A. L. *Inorg. Chem.* **2000**, *39*, 5591−5602.
(25) Boukhalfa, A.; Crumbliss, A. L. *Inorg. Chem.* **2000**, *39*, 4318−4331.
(26) Boukhalfa, A.; Crumbliss, A. L. *BioMetals* **2002**, *15*, 325−339.

binding sites of phytosiderophores,[28,29] this study is of importance for a deeper knowledge of the competition for iron(III) between the catecholate[30,31] or hydroxamate bacterial[32,33] and fungal siderophores[34−36] and the α-hydroxycarboxylate phytosiderophores,[37−39] in terms of stability and lability of their ferric species.

Experimental Section

Strain and Culture Medium. *Azotobacter vinelandii* strain D (CCM 289) was grown in aerobic conditions. The culture medium had the following composition per liter: K_2HPO_4, 1 g; $MgSO_4 \cdot 7H_2O$, 0.2 g; $CaCO_3$, 1 g; NaCl, 0.2 g; mannitol, 10 g. It was adjusted to pH 7.0 before sterilization using a 6.0 N aqueous hydrochloric acid solution. The bacteria were grown aerobically at 25 °C in 4 2-L conical flasks each containing 0.5 L of culture medium and subject to mechanical agitation for 6−7 days as previously described.[4]

Preparation of Azotobactin. After centrifugation (1000 g, 30 min 4 °C) and filtration (0.22 μm pore size, Minitan filtration unit; Millipore, Molsheim, France), the bacterial supernatant was acidified to pH 3.5 with formic acid and pumped through a column of octadecylsilane (2.0 cm × 30 cm). The fluorescent material retained by the column was rinsed with acidified distilled water (adjusted to pH 3.5 with acetic acid) and then eluted with 500 mL of 50% (v/v) acetonitrile in 0.05 M pyridine/acetic acid pH 5.0, concentrated, and lyophilized to yield 250 mg of crude azotobactin. A 244 mg (0.17 mM) portion of crude azotobactin thus obtained was kept 3 days in 10 mL of acidified water (pH adjusted to 3.0) and treated with 3 equiv of ferric chloride (0.52 mM added as a 2 M solution of ferric chloride). After 1 h at room temperature, the mixture was chromatographed on an ODS column (1.5 cm × 15 cm) which was washed first with acidified distilled water (adjusted to pH 3.5 with acetic acid in order to remove the excess of iron chloride), and then with a 1:1 mixture of acetonitrile−0.05 M pyridine/acetic acid buffer pH 5.0 which eluted the azotobactin ferric complexes (190 mg, 77%). The bulk of the complexes was evaporated to almost dryness and dissolved in 1 mL of 2 M pyridine/acetic acid buffer pH 5.0. The solution was diluted with water to 0.025 M and applied on a DEAE-Sephadex A-25 column (2.0 cm × 20 cm) eluted first isocratically with 100 mL of 0.025 M pyridine/acetic acid buffer (pH 5.0) and then with three successive linear gradients of pyridine/acetic acid pH 5.0 buffers (0.025 M to 0.05 M, 2 × 125 mL; 0.05 M to 0.1 M, 2 × 125 mL; 0.1 M to 0.5 M, 2 × 125 mL, and finally, 0.5 M to 2 M, 2 × 125 mL) yielding azotobactin δ ferric complex (112 mg) and azotobactin D ferric complex (80 mg). Azotobactin δ Fe(III) complex was purified by preparative reverse-phase HPLC (column 2.24 cm × 25 cm, ODS nucleosil 5μ) monitored spectrophotometrically at 412 nm, and eluted with 0.025 pyridine/acetic acid pH 5.0 containing 4% (v/v) acetonitrile at a flow rate of 8 mL × min^{-1} at 30 °C. Pure azotobactin δ Fe(III) complex (67 mg) was obtained after lyophilization.

Decomplexation of the Azotobactin δ Fe(III) Complex. A suspension of pure azotobactin δ Fe(III) complex (30 mg in 40 mL 0.2 M solution of EDTA disodium salt) was stirred for 1 h, diluted twice with water at pH 4.0, and chromatographed on a reverse-phase column ODS (2 cm × 15 cm) made up in 0.1 M EDTA pH 4.0. The column was first washed with 50 mL of a 0.1 M solution of EDTA, and then with 300 mL of water at pH 4.0. Azotobactin was eluted as its free ligand with a 1:1 mixture (v/v) of acetonitrile in 0.05 M pyridine/acetic acid pH 5.0, lyophilized, and applied to and eluted from a DEAE-Sephadex A-25 column with a linear gradient of pyridine/acetic acid pH 5.0 (0.05 M to 0.5 M, 2 × 0.3 L). Pure azotobactin δ free ligand (22 mg) was lyophilized and stored desiccated in the dark at −20 °C.

Potentiometry and Spectrophotometry. The solutions were prepared with deionized water, and the ionic strength was fixed, using 0.1 M sodium perchlorate (Merck, p.a.). Azotobactin δ or its ferric complex was dissolved and introduced into a jacketed cell (20 mL) maintained at 25.0 ± 0.1 °C using a Haake FJ thermostat. The initial concentrations were calculated using the molar absorptivities[4] determined at p[H] = 5.00 for free azotobactin δ ($\epsilon_{380} = 23.5 \times 10^3$ M^{-1} cm^{-1}, $\epsilon_{366} = 19.6 \times 10^3$ M^{-1} cm^{-1}) and for azotobactin δ iron(III) complex ($\epsilon_{412} = 23.0 \times 10^3$ M^{-1} cm^{-1}, $\epsilon_{540} = 10.0 \times 10^3$ M^{-1} cm^{-1}, $\epsilon_{550} = 2.0 \times 10^3$ M^{-1} cm^{-1}). The solutions were deoxygenated and flushed continuously with argon during the titrations, in order to prevent oxidation[28] of the catechol group of azotobactin δ. The free hydrogen concentrations were measured with an Ag/AgCl combined glass electrode (Tacussel, High Alkalinity, filled with saturated NaCl and AgCl traces) and a Tacussel Isis 20 000 millivoltmeter. Standardization of the millivoltmeter and verification of the linearity of the electrode (3.00 < p[H] < 9.00) were performed using commercial Merck buffered solutions (p[H] = 4.00, 7.00, and 9.00) according to classical methods.[40,41] The titrations of the free siderophore (≈ 10^{-4} M, 2.60 < p[H] < 10.00) and of its iron(III) species (≈ 0.5 × 10^{-4} M, 1.00 < p[H] < 5.50) were carried out by addition of known volumes of either sodium hydroxide (0.1 M, Merck, Titrisol) or hydrochloric acid (0.1 M, Merck, Titrisol) with a piston-fitted microburet (Manostat). When equilibrium conditions were reached, absorption spectra were measured on small samples (0.5 mL) at different p[H] values. The spectrophotometric measurements were recorded using a Kontron Uvikon 860 spectrophotometer between 250 and 650 nm using a 0.2 cm quartz optical cell (Hellma). An example of the spectral changes of free azotobactin δ (7.5 × 10^{-5} M) and its ferric complex (1.6 × 10^{-4} M) as a function of hydrogen ion concentrations is given in Figure 2.

The potentiometric data obtained during the potentiometric titrations were fitted with the commercial Miniquad[42] software which calculates protonation constants using an iterative least-

(27) Albrecht-Gary, A. M.; Blanc, S.; Rochel, N.; Ocaktan, A. Z.; Abdallah, M. A. *Inorg. Chem.* **1994**, *33*, 6391−6402.
(28) Raymond, K. N.; Müller, G.; Matzanke, B. F. *Top. Curr. Chem.* **1984**, *123*, 49−102.
(29) Albrecht-Gary, A. M.; Crumbliss, A. L. In *Iron Transport and Storage in Microorganisms, Plants and Animals*; Siegel, H., Ed.; Metal Ions in Biological Systems 35; Marcel Dekker: New York, 1998; pp 239−327.
(30) Pollack, J. R.; Neilands, J. B. *Biochem. Biophys. Res. Commun.* **1970**, *38*, 989−992.
(31) Persmark, M.; Neilands, J. B. *BioMetals* **1992**, *5*, 29−36.
(32) O'Brien, I. G.; Gibson, F. *Biochim.* Biophys. Acta **1970**, *215*, 393−402.
(33) Bickel, M.; Bosshardt, R.; Gäumann, E.; Reusser, P.; Vischer, E.; Voser, W.; Wettstein, A.; Zähner, H. *Helv. Chim. Acta* **1960**, *43*, 2118−2128.
(34) Neilands, J. B. *J. Am. Chem. Soc.* 19**5**2, *74*, 4846−4847.
(35) Moore, R. E.; Emery, T. *Biochemistry* **1976**, *15*, 2719−2723.
(36) Keller-Schierlein, W.; Diekmann, H. *Helv. Chim. Acta* **1970**, *53*, 2035−2044.
(37) Sugiura, Y.; Tanaka, H.; Mino, Y.; Ishida, T.; Ota, N.; Inoue, M.; Nomoto, K.; Yoshioka, H.; Takemoto, T. *J. Am. Chem. Soc.* **1981**, *103*, 6979−6982.
(38) Smith, M. J.; Neilands, J. B. *J. Plant. Nutr.* **1984**, *7*, 449−458.
(39) Fushiya, S.; Sato, Y.; Nozoe, S.; Nomoto, K.; Takemoto, T.; Takagi, S. I. *Tetrahedron Lett.* **1980**, *21*, 3071−3072.
(40) Hider, R. C. *Struct. Bonding* **1984**, *58*, 25−88.
(41) Martell, A. E.; Motekaitis, R. J. In *Determination and Use of Stability Constants*; VCH: Weinheim, 1988; Chapter 1, pp 7−19.
(42) Sabatini, A.; Vacca, A.; Gans, P. *Talanta* **1974**, *21*, 53−77.

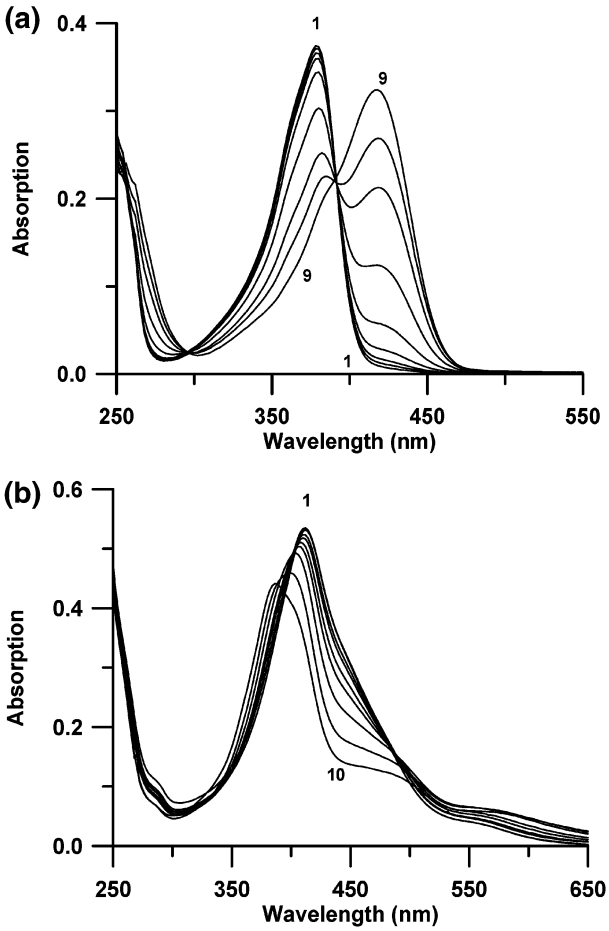

Figure 2. Spectrophotometric titration of azotobactin δ and its ferric complex as a function of p[H]. Solvent: water; $I = 0.1$; $T = 25.0(1)$ °C; $l = 0.2$ cm; (a) [azotobactin δ]$_{tot} = 7.5 \times 10^{-5}$ M, [HCl]$_0 = 1 \times 10^{-3}$ M. Spectra 1−9: p[H] = 3.51; 4.00; 4.59; 5.00; 5.42; 6.01; 6.50; 6.98; 7.51. (b) [azotobactin δ]$_{tot} = 1.6 \times 10^{-4}$ M, [iron(III)]$_{tot} = 1.6 \times 10^{-4}$ M, [HCl]$_0$ = 0.1 M. Spectra 1−10: p[H] = 4.90; 4.54; 4.07; 3.22; 3.03; 2.72; 2.51; 2.19; 1.98; 1.68.

squares Gauss−Newton method of refinement. The simultaneous potentiometric and spectrophotometric data recorded at various p[H] values for azotobactin δ in the presence or absence of iron(III) were fitted with the Letagrop-Spefo program[43,44] which adjusts the absorptivities and the stability constants of the species formed at equilibrium. It uses the Newton−Raphson algorithm to solve mass balance equations and a "pit-mapping" method to minimize the errors and determine the best values for the parameters.

Electrochemistry. Cyclic voltammetry measurements were performed using a GSTP3 (Tacussel) triangular signal generator, a PRG5 (Tacussel) potentiostat and, a D15 (Tektronix) memory oscilloscope as recording instrument. These experiments were carried out in a three electrode cell using a hanging mercury drop working electrode (Metrohm), a platinum wire auxiliary, and a saturated calomel reference electrode (Tacussel). Cyclic voltammograms were recorded between −200 and −1200 mV/SCE at scan rates ranging from 50 mV to 10 V s^{-1}. All the solutions were prepared in boiled deionized water with sodium perchlorate as supporting electrolyte (0.1 M, Prolabo, Rectapur). Azotobactin δ ferric solutions (10^{-4} M) were prepared by weight, and exact concentrations were determined after measuring their absorption spectrum at p[H] = 5.00 as performed for potentiometric and spectrophotometric measurements. Proton concentrations were measured using a Tacussel Isis 20000 millivoltmeter using a Ag/AgCl combined glass electrode (Tacussel, High Alkalinity, filled with saturated NaCl solution), and standardization was performed with Merck buffers (p[H] = 4.00 and 7.00). The p[H] was fixed with a tris(hydroxymethyl-methylamine) (0.04 M, Merck, p.a.)/maleic acid (0.04 M, Merck) buffer as it has no electroactivity in the potential range studied and does not form any iron complex. p[H] values varied between 5.00 and 8.75 by the addition of small volumes (piston-fitted microburet Manostat) of sodium hydroxide (1 M, Merck, Titrisol). Buffered solutions were maintained at a constant temperature 25.0(1) °C and flushed with water-saturated argon.

Circular Dichroism. CD spectra were measured on an Isa Jobin Yvon CD6 spectropolarimeter using a 1 cm quartz optical cell (Hellma). All solutions were prepared with deionized water and maintained at 25.0(1)°C. The p[H] of the stock solutions of free azotobactin δ samples (4.36×10^{-5} M) was fixed at 1.50 using perchloric acid (Merck, Suprapur), and the p[H] value of the azotobactin iron(III) complex aqueous solutions was found to be 5.80. Protons, ligand, and iron(III) azotobactin concentrations were determined as for potentiometric, spectrophotometric, or electrochemical measurements.

Kinetic Measurements. Formation and dissociation of azotobactin δ iron(III) complex required the use of rapid mixing techniques, and the kinetics were recorded on a Durrum-Gibson or a sequential Applied Photophysics stopped flow DX17MV spectrofluorimeter. Data were then treated on line using the Biokine program[45] which fits up to three exponential functions to the experimental curves with the Simplex algorithm[46] after initialization with the Padé−Laplace method.[47] All solutions were prepared with deionized water at fixed ionic strength (2.0 M, $NaClO_4$, Merck, p.a.) and maintained at 25.1 ± 0.1 °C.

Formation kinetics were studied in the 1.31−2.21 p[H] range in the presence of an excess of iron(III) (9.6×10^{-5} M < [Fe(III)] < 4.79×10^{-4} M). The stock iron(III) solutions ($FeCl_3$, $6H_2O$, Merck, p.a.), prepared in acidic conditions, were previously back-titrated with thorium nitrate solution (10^{-2} M, Merck, p.a.) in the presence of excess EDTA (10^{-2} M, Merck, Titriplex III) with xylenol orange (Merck) as indicator. Free azotobactin δ solutions (8×10^{-6} M) were prepared with deionized degassed water and maintained under argon to avoid the oxidation of the catechol group. The reaction was monitored spectrophotometrically at 412 nm, the maximum absorption of the ferric complex (Figure 2).

Acid dissociation kinetics were monitored by spectrophotometry at 412 nm maximum absorption of ferric azotobactin δ (Figure 2) using 1 cm path length cuvettes, and also by fluorescence spectroscopy at 380 nm excitation wavelength, maximum absorption of free azotobactin δ (Figure 2) using 0.2 cm path length cuvettes. The kinetics traces between 350 and 520 nm were recorded every 10 nm for [H$^+$] = 0.052 M using absorption detection. For [H$^+$] = 0.042 M, the excitation wavelength was varied between 300 and 410 nm. For fluorimetric detection, KV 418 filter (Schott, wavelength cut at 418 nm) was used, and the ferric solutions (9×10^{-6} M) were filtered on Millipore filter (Ø = 0.22 μm, GS). For the spectrophotometric detection, azotobactin δ iron(III) complex concentration was 2.0×10^{-5} M. In each case, the initial p[H] was 5.80(0.05), and titrated perchloric acid solutions (70%, Merck, p.a.)

(43) Sillen, L. G.; Warnqvist, B. *Ark. Kemi* **1968**, *31*, 377-390.
(44) Arnek, R.; Sillen, L. G.; Wahlberg, O. *Ark. Kemi* **1968**, *31*, 353-363.
(45) Bio-logic Company, Echirolles, France, 1991.
(46) Nelder, J. A.; Mead, R. *Comput. J.* **1965**, *7*, 308−313.
(47) Yeramian, E.; Claverie, P. *Nature* **1987**, *326*, 169−174.

Table 1. Deprotonation Constants of Azotobactin δ and Stability Constants of Its Ferric Complexes[a]

equilibrium	thermodynamic constant (σ)
$LH^{4-} \rightleftarrows L^{5-} + H^+$	$pK_1 > 11$[c]
$LH_2^{3-} \rightleftarrows LH^{4-} + H^+$	$pK_2 = 10.8(1)$[b]
	$pK_2 = 10.8(1)$
$LH_3^{2-} \rightleftarrows LH_2^{3-} + H$	$pK_3 = 8.4(2)$[b]
$LH_4^- \rightleftarrows LH_3^{2-} + H^+$	$pK_4 = 6.4(0.2)$[b]
	$pK_4 = 6.3(1)$
$LH_5 \rightleftarrows LH_4^- + H^+$	$pK_5 = 4.2(1)$[b]
$LH_6^+ \rightleftarrows LH_5 + H^+$	$pK_6 = 3$[d]
$LH^{4-} + Fe(III) \rightleftarrows LFe(III)^{2-} + H^+$	$\log \beta_{LFe} = 23.9(2)$
$LH^{4-} + Fe(III) + \rightleftarrows LHFe(III)^-$	$\log \beta_{LHFe} = 28.1(1)$
$LH^{4-} + Fe(III) + H^+ \rightleftarrows LH_2Fe(III)$	$\log \beta_{LH_2Fe} = 31.1(1)$
$LH^{4-} + Fe(III) + 2H^+ \rightleftarrows LH_3Fe(III)^+$	$\log \beta_{LH_3Fe} = 33.1(1)$

[a] Solvent: water; $I = 0.1$; $T = 25.0(1)$ °C; potentiometry and spectrophotometry. [b] Potentiometric measurements. [c] Reference 53. [d] References 51 and 52.

from 3.1×10^{-3} M to 1.0 M were used for the acid dissociation of azotobactin δ ferric complexes.

Results

Azotobactin δ Acido-Basic Species. Azotobactin δ has five protonation sites involved in the binding of iron(III): the two hydroxyl groups of the catechol group of the chromophore, the hydroxyl group of the C-terminal hydroxamate group, and finally both the carboxyl and the hydroxyl functions of the central α-hydroxy carboxylic acid. The sixth protonation site belongs to the aspartic acid located on the peptidic chain (Figure 1). The positive charge of the fully protonated form of azotobactin δ, denoted LH_6^+, occurs from the chromophore. The deprotonation constants of azotobactin δ and the stability constants of its ferric complex are presented in Table 1.

By comparison with the closely related chromophore of pyoverdin PaA[27] ($pK = 10.8(3)$ and $pK = 5.7(2)$), we easily assigned K_2 and K_4 to the two protonation sites of the dihydroxyquinoline moiety of azotobactin δ ($pK_2 = 10.8(1)$, $pK_4 = 6.4(2)$). $pK_3 = 8.4(2)$ is a classical value for hydroxamic acids.[28,29,48−50] The $pK_5 = 4.2(1)$ value which was found to be identical to the first deprotonation constant of ferric azotobactin δ ($\log \beta_{LHFe} - \log \beta_{LFe} = 4.2(3)$) could easily be assigned to aspartic acid, which is not involved in the coordination of the ferric cation. In order to prevent the oxidation of the catechol-type moiety of azotobactin δ, we used a p[H] range between 2.6 and 10.0 which did not allow the determination of the pK_1 and pK_6 values. Therefore, we used the value $pK_6 = 3$ reported by Jenkins[51] and confirmed by Pearce and Creamer[52] for the deprotonation of the carboxylic function of the central α-hydroxycarboxylic acid (Figure 1). It was not possible to determine pK_1 in agreement with the literature[53] which reports very high protonation constants (>11) for the hydroxyl group of the α-hydroxycarboxylic function.

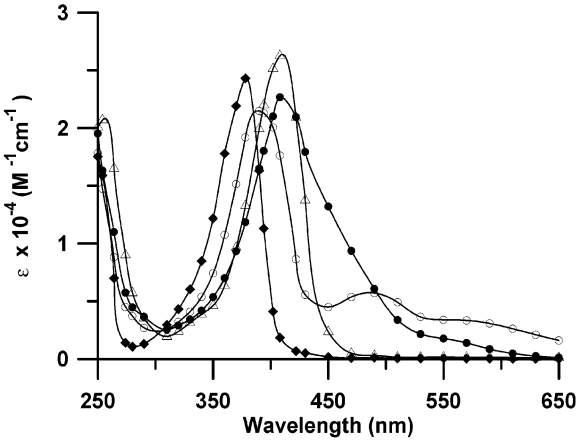

Figure 3. Calculated electronic spectra of the different protonated azotobactin δ species and its ferric complex: (◆) $\epsilon_{LH_6^+} = \epsilon_{LH_5} = \epsilon_{LH_4^-}$, (△) $\epsilon_{LH_3^{2-}} = \epsilon_{LH_2^{3-}}$, (●) $\epsilon_{LFe^{2-}} = \epsilon_{LHFe^-} = \epsilon_{LH_2Fe}$, (○) $\epsilon_{LH_3Fe^+}$. Solvent: water; $I = 0.05$; $T = 25.0(1)$ °C.

Azotobactin δ forms three different absorbing species corresponding to the di-, the mono-, and the deprotonated form of the chromophore. Taking into account the pK values presented in Table 1, it was deduced that LH_2^{3-} and LH_3^{2-} should have the same electronic spectra corresponding to the monoprotonated form of the chromophore, and that LH_4^-, LH_5, and LH_6^+ should show the same absorption spectrum corresponding to the diprotonated form of the chromophore. Processing the simultaneously determined potentiometric and spectrophotometric data with the Letagrop-Spefo program,[43,44] the pK_2 and pK_4 values were obtained in excellent agreement with the potentiometric measurements. The corresponding electronic spectra are presented in Figure 3. However in our experimental conditions, it was not possible to calculate the electronic spectra of L^{5-} and LH^{4-} which correspond to the deprotonation of the chromophore of azotobactin δ.

Azotobactin δ Ferric Complexes. The different species of the azotobactin δ ferric complex were characterized by absorption spectrophotometry while varying the p[H]. Two LMCT bands at 440−490 nm and 540−550 nm were observed related, respectively, to the dihydroxyquinoline and the hydroxamate binding sites (Figure 3). From the potentiometric data, it was concluded that the two hexacoordinated complexes, namely LFe^{2-} and $LHFe^-$, involving the binding of the α-hydroxycarboxylic acid bidentate group, and differing only from the state of protonation of the aspartic acid moiety external to the coordination sites, should show an identical electronic spectrum (Figure 3). No significant changes in the absorption properties were observed upon protonation of the carboxylic site of the α-hydroxycarboxylic function ($LHFe^-$). More significant changes appear when the latter was diprotonated (LH_2Fe).

Redox Potentials. Reversible electrochemical systems in the range of p[H] values between 6.75 and 7.75 at 0.1 V s^{-1} potential scan rate were observed. The reduction potentials measured under these conditions were found to be $[H^+]$ independent, and the calculated average value was equal to −390(± 5) mV (NHE). As an example, a cyclic voltammogram is given in Figure S1 (Supporting Information).

(48) Exner, O.; Simon, W. *Collect. Czech. Chem. Commun.* **1965**, *30*, 4078−4093.
(49) Brink, C. P.; Crumbliss, A. L. *J. Org. Chem.* **1982**, *47*, 1171−1176.
(50) Brink, C. P.; Fish, L. L.; Crumbliss, A. L. *J. Org. Chem.* **1985**, *50*, 2277−2281.
(51) Jenkins, T. W. *J. Biol. Chem.* **1961**, *234*, 1121−1125.
(52) Pearce, K. N.; Creamer, L. K. *Aust. J. Chem.* **1975**, *28*, 2409−2415.
(53) Migal, P. K.; Sychev, A. Ya. *Zh. Neorg. Khim.* **1958**, *3*, 314−324.

Table 2. UV−Vis and CD Properties of Different Siderophores in Water

siderophore	UV−vis λ_{max} (nm) (ϵ_{max} (M^{-1} cm^{-1}))	CD bands λ_{ext} (nm) ($\Delta\epsilon$ (M^{-1} cm^{-1})) Δ	CD bands λ_{ext} (nm) ($\Delta\epsilon$ (M^{-1} cm^{-1})) Λ
azotobactin δ	412 (1) (23 000 (200)) shoulder at 440 (14 000 (200)) shoulder at 540 (2600 (200))		330(4) (− 5.1(1)) 380(10) (−1.6(2)) 416(5) (− 3.1(2)) 480(8) (2.5(1)) shoulder at 550 (0.6(0))
desferriferrichrome[54]	425 (2895)		360 (−3.7) 465 (2.4)
desferriferrichrome A[55]	440 (3360)		330 (−3.9) q 465 (3.2)
desferriferricrocin[56]	434 (2460)		290 (−3.78) 360 (−1.62) 450 (2.47)
coprogen[56]	434 (2820)	375 (2.1) 474 (−1.26)	
alcaligin[91]			shoulder at 300 (−2.5) 370 (−4.4) 450 (+4.3)
enterobactin[57]	495 (5600)	420 (4.0) 535 (−4.0)	
TRAM[92]	502 (4650)	432 (4.2) 550 (−2.3)	
L-enterobactin model[93]	495 (5200)		535 (3.0)
D-enterobactin analog[93]	495 (5600)	535 (−3.0)	
L-parabactin[94]	520 (3100)		550 (2.2)
L-parabactin A[94]	522 (3320)		550 (1.2)
D-parabactin A[94]	522 (3320)	550 (−1.2)	
pseudobactin[6]	400 (15 000)		400 (2.0) 436 (−0.8) 502 (0.3)
pyoverdin G4R[14]	400 (19 500) shoulder at 460 (6000) shoulder at 540 (3000)		400 (1.7) 460 (−0.8) 540 (−0.3)

Circular Dichroism. The CD spectrum of azotobactin δ was previously reported, showing three negative Cotton effects, respectively, at 327 nm ($\Delta\epsilon = -1.6$ M^{-1} cm^{-1}), 377 nm ($\Delta\epsilon = -0.8$ M^{-1} cm^{-1}), and 460 nm ($\Delta\epsilon = -0.02$ M^{-1} cm^{-1}) and one very slightly positive Cotton effect at 420 nm ($\Delta\epsilon = +0.15$ M^{-1} cm^{-1}).[4] Since it is very different from the spectrum of pseudobactin B 10 in the UV−vis region,[6] the absolute configuration of the carbon atom C-11 adjacent to the chromophore had to be established by degradation methods and found to be (S) like its homologue in pseudobactin B 10.[4]

The CD spectrum of the azotobactin δ ferric complex presents two negative Cotton effects in the UV−vis region, respectively, at 327 nm ($\Delta\epsilon = -5.1$ M^{-1} cm^{-1}) and 417 nm ($\Delta\epsilon = -3.2$ M^{-1} cm^{-1}) and two positive Cotton effects in the visible, the first at 480 nm ($\Delta\epsilon = +2.5$ M^{-1} cm^{-1}) and the second with a lower intensity at 565 nm ($\Delta\epsilon = +0.6$ M^{-1} cm^{-1}) (Figure 4). From the comparison of UV−vis and CD spectra (Table 2), it was possible to assign these bands, respectively, to hydroxamate−Fe(III) and catecholate−Fe(III) charge-transfer bands as assigned for the corresponding absorption spectra. This is in agreement with the reported CD spectra of trishydroxamate complexes (ferrichrome,[54] ferrichrome A,[55] ferricrocin,[56] coprogen[56]) which show positive Cotton effects between 450 and 474 nm (Table 2)

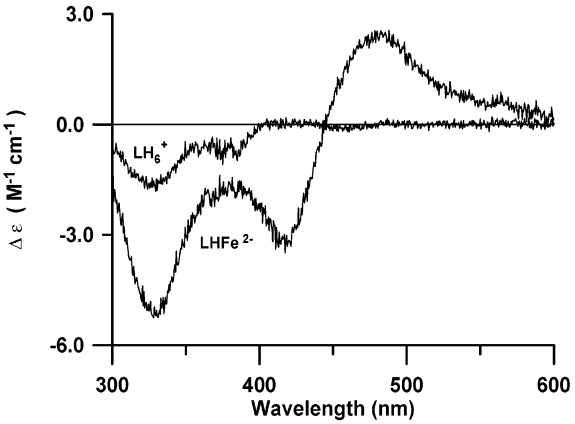

Figure 4. Circular dichroism of free azotobactin δ and its ferric complex. Solvent: water; $T = 25.0(1)$ °C.

and of enterobactin−Fe(III) complex[57] which shows an intense negative Cotton effect at 535 nm (Table 2). Very slight differences between the wavelength maxima or minima determined either by CD or by UV−vis were observed, very certainly due to experimental errors in their determination, as observed in other siderophore CD studies as well (Table 2). The minimum measured at 416 nm on the CD spectra of ferric azotobactin δ complex could be assigned to the chromophore absorption localized at 412 nm (but it is also possible that many bands exist below 450 nm).

No characteristic charge-transfer band corresponding to catecholate−Fe(III) was apparent for ferric pseudobactin,[6]

(54) van der Helm, D.; Baker, J. R.; Eng-Wilmot, D. L.; Hossain, M. B.; Loghry, R. A. *J. Am. Chem. Soc.* **1980**, *102*, 4224−4231.
(55) Abu-Dari, K.; Raymond, K. N. *J. Am. Chem. Soc.* **1977**, *99*, 2003−2005.
(56) Wong, G. B.; Kappel, M. J.; Raymond, K. N.; Matzanke, B.; Winkelmann, G. *J. Am. Chem. Soc.* **1983**, *105*, 810−815.
(57) Rodgers, H. J.; Synger, C.; Kimber, B.; Bayley, P. M. *Biochim. Biophys. Acta* **1977**, *497*, 548−557.

and only a shoulder of weak intensity was observed for azotobactin δ. The charge-transfer band due to hydroxyacid−Fe(III) is localized in the UV region and has a low intensity. This is the reason the corresponding CD band could not be detected as in the case of aerobactin,[58] and why the CD spectrum of azotobactin δ ferric complex is very similar to those of ferric trishydroxamate complexes.

Azotobactin δ Ferric Complex Formation Kinetics. During the formation of azotobactin δ in acidic medium, a single-exponential signal in 20 s without any loss of signal amplitude during the mixing time (3 ms) was observed. The variations of the pseudo-first-order rate constant with iron and proton concentrations are presented in Figure 5 and fit with the mathematical eqs 1−3:

$$k_{obs} = k_a[Fe(III)]_{tot} + k_b[Fe(III)]_{tot}^2 \quad (1)$$

$$k_a = (a_1[H^+] + a_2)/([H^+] + a_3)([H^+] + a_4) \quad (2)$$

$$k_b = (b_1[H^+] + b_2)/([H^+] + b_3)([H^+] + b_4) \quad (3)$$

Under the conditions used, azotobactin δ exists in two forms: LH_5 and LH_6^+, the iron(III) species in solution being essentially Fe^{3+} and $FeOH^{2+}$. However, the dependence of the rate constant on $[Fe(III)]^2_{tot}$ indicates that the reactivity of the dimer $Fe_2(OH)_2^{4+}$ has to be taken into account, and the following mechanism can thus be deduced: The rate law

$$Fe^{3+} + LH_6^+ \xrightarrow{k_1} LH_5Fe^{3+} + H^+ \quad (4)$$

$$Fe^{3+} + LH_5 \xrightarrow{k_2} LH_5Fe^{3+} \quad (5)$$

$$Fe(OH)^{2+} + LH_6^+ \xrightarrow{k_3} LH_5Fe^{3+} + H_2O \quad (6)$$

$$Fe(OH)^{2+} + LH_5 \xrightarrow{k_4} LH_5Fe^{3+} + OH^- \quad (7)$$

$$Fe_2(OH)_2^{4+} + LH_6^+ \xrightarrow{k_5} LH_5Fe^{3+} + Fe(OH)^{2+} + H_2O \quad (8)$$

$$Fe_2(OH)_2^{4+} + LH_5 \xrightarrow{k_6} LH_5Fe^{3+} + Fe(OH)^{2+} + OH^- \quad (9)$$

$$LH_6^+ \overset{K_{6,rapid}}{\rightleftharpoons} LH_5 + H^+ \quad (10)$$

$$Fe(H_2O)_6^{3+} \overset{K_{H,rapid}}{\rightleftharpoons} Fe(H_2O)_5(OH)^{2+} + H^+ \quad (11)$$

$$2Fe(H_2O)_6^{3+} \overset{K_{D,rapid}}{\rightleftharpoons} Fe_2(H_2O)_{10}(OH)_2^{4+} + 2H^+ \quad (12)$$

relative to LH_5 and LH_6^+ is

$$-\frac{d([LH_6^+] + [LH_5])}{dt} = k_1[Fe^{3+}][LH_6^+] + k_2[Fe^{3+}][LH_5] + k_3[Fe(OH)^{2+}][LH_6^+] + k_4[Fe(OH)^{2+}][LH_5] + k_5[Fe_2(OH)_2^{4+}][LH_6^+] + k_6[Fe_2(OH)_2^{4+}][LH_5]$$

$$-\frac{d([LH_6^+] + [LH_5])}{dt} = k_{obs}([LH_6^+] + [LH_5])$$

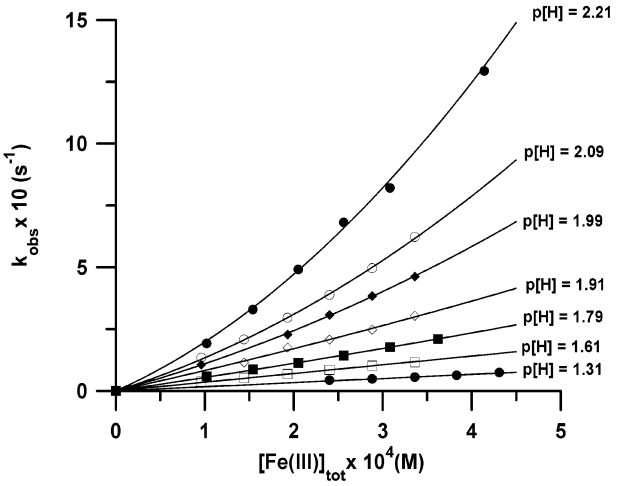

Figure 5. Formation of the azotobactin δ ferric complex: variation of the pseudo-first-order rate constant versus total iron(III) and proton concentrations. Solvent: water; $I = 2$; $T = 25.0(2)$ °C; $l = 2$ cm; c_{tot} = [azotobactin δ] = 8×10^{-6} M.

Considering that the total concentration of free azotobactin δ is $[L]_{tot} = ([LH_5] + [LH_6^+])$, using the expression of K_6 gives $[LH_5] = [H^+][L]_{tot}/([H^+] + K_6)$ and $[LH_6^+] = K_6[L]_{tot}/([H^+] + K_6)$. Since the concentrations $[Fe_2(OH)_2^{4+}]$ and $[Fe(OH)^{2+}]$ are very small under our conditions and can be neglected, the total concentration of iron(III) becomes

$$[Fe(III)]_{tot} = [Fe^{3+}] \times ([H^+] + K_H)/[H^+] \quad (13)$$

The concentration of all the different iron(III) species as a function of the total iron(III) concentration can be thus calculated

$$[Fe^{3+}] = [Fe(III)]_{tot} \times [H^+]/([H^+] + K_H) \quad (14)$$

$$[Fe(OH)^{2+}] = [Fe(III)]_{tot} \times K_H/([H^+] + K_H) \quad (15)$$

$$[Fe_2(OH)_2^{4+}] = [Fe(III)]_{tot} \times K_D/([H^+] + K_H)^2 \quad (16)$$

Using all these equations, the new expression of the rate law becomes

$$v = \left\{\frac{k_1[H^+]^2 + (k_2K_6 + k_3K_H)[H^+] + k_4K_HK_6}{([H^+] + K_H)([H^+] + K_6)}\right\}[Fe(III)]_{tot}[L] + \left\{\frac{k_5K_D[H^+] + k_6K_DK_6}{([H^+] + K_H)^2([H^+] + K_6)}\right\}[Fe(III)]^2_{tot}[L] \quad (17)$$

We were unable to determine k_1 and k_5. However, k_4 (2.1(0.3) $\times 10^4$ M^{-1} s^{-1}) and k_6 (6.1(0.3) $\times 10^5$ M^{-1} s^{-1}) could be obtained. For the expression $k_2 \times K_6 + k_3K_H = 8.8(0.6)$ s^{-1}, K_6 is approximately equal to K_H (10^{-3} M).[59] Furthermore, $Fe(OH)^{2+}$ is much more reactive than Fe^{3+} ($k_3 \gg k_2$). It can therefore be written that $k_3K_H \gg k_2K_6$. This allows the determination of $k_3 = 5.9(0.4) \times 10^3$ M^{-1} s^{-1}.

(58) Harris, W. R.; Carrano, C. J.; Raymond, K. N. *J. Am. Chem. Soc.* **1979**, *101*, 2722−2727.

(59) Milburn, R. M.; Vosburgh, W. C. *J. Am. Chem. Soc.* **1955**, *77*, 1352−1355.

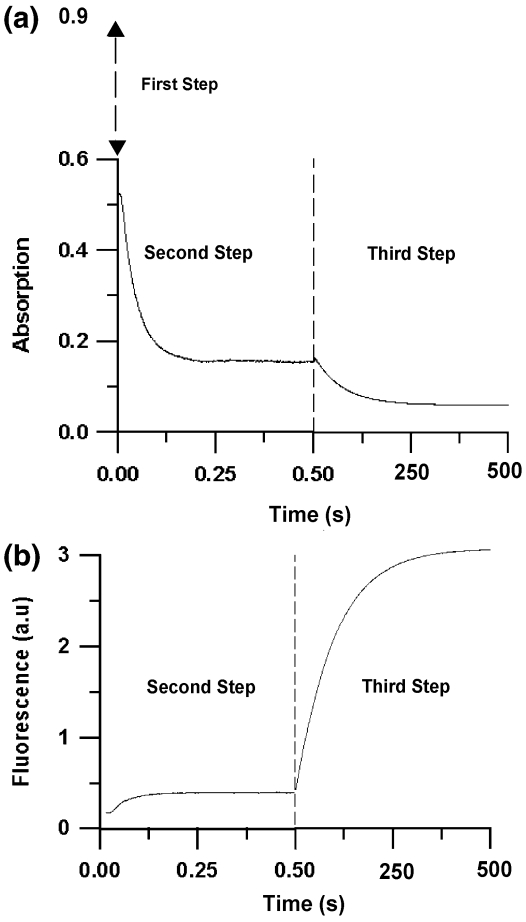

Figure 6. Dissociation kinetics of azotobactin δ ferric species. Solvent: water; $I = 2$; $T = 25.0(2)$ °C. (a) [azotobactin δ Fe(III)]$_{tot} = 2.0 \times 10^{-5}$ M, [H$^+$] = 0.057 M, $l = 2$ cm; $\lambda = 412$ nm. (b) [azotobactin δ Fe(III)]$_{tot} = 8.5 \times 10^{-6}$ M, [H$^+$] = 0.059 M, $l = 2$ mm, $\lambda_{exc} = 380$ nm.

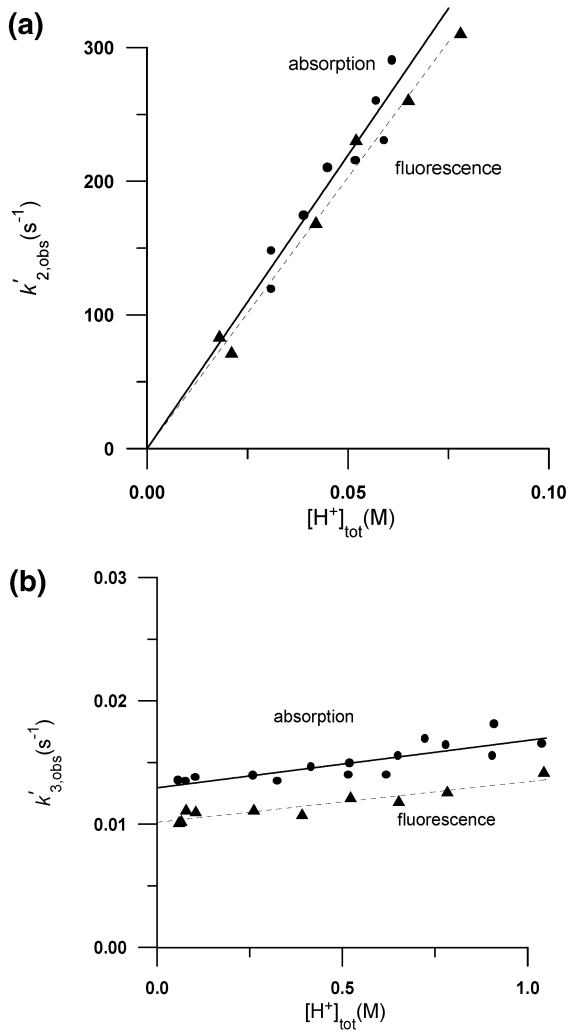

Figure 7. Variation of the pseudo-first-order constants for the acidic dissociation of ferric azotobactin δ with proton concentration by (a) absorption and (b) fluorescence measurements. Solvent: water; $I = 2.0$ M; $T = 25.0(2)$ °C. The errors are estimated to 2σ for the kinetic constants.

Dissociation Kinetics. 30% of the total absorption intensity has been lost during the mixing of the reactants. This indicates that one or several rapid steps took place before the beginning of the recording (<5 ms). Two other steps were determined in our conditions using fluorescence and absorption spectrophotometry: one on a 50 ms and the other a 500 s time scale (Figure 6).

The variation of the two corresponding pseudo-first-order constants $k_{2,obs}$ and $k_{3,obs}$ with [H$^+$] is given in Table S1 (Supporting Information). Both vary linearly with the concentrations of protons and correspond to the following expressions:

$$k_{2,obs} = a[H^+] \tag{18}$$

$$k_{3,obs} = b[H^+] + c \tag{19}$$

The a (Figure 7a) and average values of b and c (Figure 7b) were determined: $a = 4.63(0.04) \times 10^3$ M^{-1} s^{-1}, $b = 3.8(0.7) \times 10^{-3}$ M^{-1} s^{-1}, and $c = 13.0(0.4) \times 10^{-3}$ s^{-1}.

The number of protons involved in the second step was determined by linearization of A'_∞, the absorption observed at the end of this reaction (see Figure 8), as a function of [H$^+$], using the Schwarzenbach equation,[60,61] where A'_0 corresponds to the absorption at the beginning of this step, A'_f to its final absorption, and K to the protonation constant of the equilibrium

$$A'_\infty = \frac{A'_0 - A'_\infty}{K[H^+]^n} + A'_f \tag{20}$$

A linear plot of A' versus $A'_\infty = A'_0 - A'_\infty/K\,[H^+]^n + A'_f$ is obtained for $n = 2$. From the slope and the intercept of the regression line (Figure 7), it was possible to calculate $K = K'_4 \times K'_5$ (see below eqs 24 and 25) equal to 1130(80) M^{-2} and $\epsilon'_f = 1000(200)$ M^{-1} cm^{-1}, corresponding to A'_f.

The data treatment of multiwavelength kinetic traces (Figure 9a) gives the spectra of the different intermediates present during this acid dissociation reaction (Figure 9b).

The electronic spectra previously determined strongly suggest that the first protonated intermediate complex is LH_3Fe^+. Then, we can assume that during the mixing time

(60) Anderegg, G.; L'Eplattenier, F.; Schwarzenbach, G. *Helv. Chim. Acta* **1963**, *46*, 1409−1422.
(61) Schwarzenbach, G.; Schwarzenbach, K. *Helv. Chim. Acta* **1963**, *154*, 1390−1400.

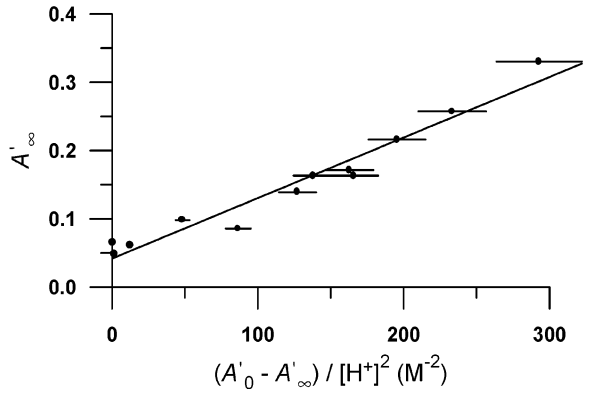

Figure 8. Variation of the absorption measured at 412 nm after the first observed dissociation step of ferric azotobactin δ complexes as a function of $[H^+]$ using $n = 2$ in the Schwarzenbach equation.[60] Solvent: water; $I = 2$; $T = 25.0$ (2) °C; $l = 2$ cm; [azotobactin δ Fe(III)]$_{tot} = 2.0 \times 10^{-5}$ M.

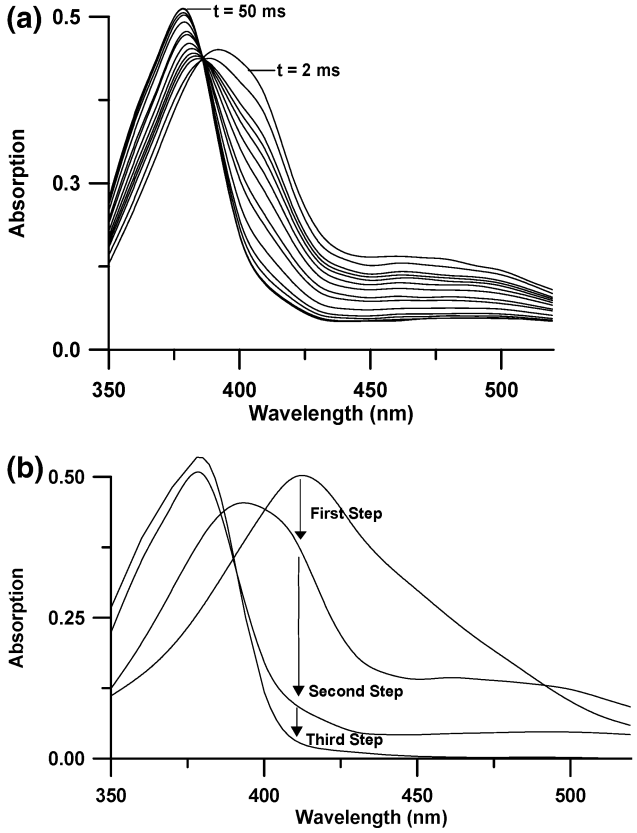

Figure 9. (a) Spectrum variation recorded during the second dissociation step of ferric azotobactin δ complexes as a function of time. (b) Calculated absorption spectra of the intermediates observed during the acid dissociation of ferric azotobactin δ complexes. Solvent: water; $I = 2$; $T = 25.0(2)$ °C; $l = 1$ cm; [azotobactin δ Fe(III)]$_{tot} = 2.2 \times 10^{-5}$ M; $[H^+] = 0.052$ M.

the following equilibria take place:

$$LFe^{2-} + H^+ \rightleftarrows LHFe^- \quad K'_1 = 1.6 \times 10^4\ M^{-1} \quad (21)$$

$$LHFe^- + H^+ \rightleftarrows LH_2Fe \quad K'_2 = 1.0 \times 10^3\ M^{-1} \quad (22)$$

$$LH_2Fe + H^+ \rightleftarrows LH_3Fe^+ \quad K'_3 = 1.0 \times 10^2\ M^{-1} \quad (23)$$

In the second step which is first order with $[H^+]$, two protons are involved in this reaction, indicating a rapid protonation step after the rate-limiting step.

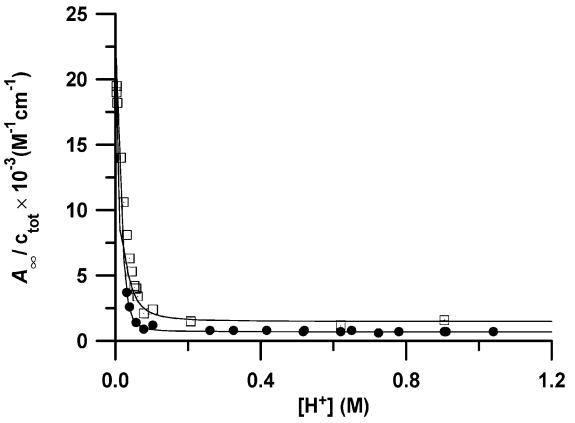

Figure 10. Variation of the absorption at the end of the second and the third dissociation steps of ferric azotobactin δ complexes (□, A'_∞, ●, A''_∞) as a function of $[H^+]$. Solvent: water; $I = 2$; $T = 25.0(2)$ °C; $l = 2$ cm; c_{tot} = [azotobactin δ Fe(III)]$_{tot} = 2 \times 10^{-5}$ M; $\lambda = 412$ nm.

From the following equations giving the rate expression $k_{2,obs} = k'_4\,[H^+]$, it could be deduced that $k'_4 = a = 4.63(4) \times 10^3\ M^{-1}\ s^{-1}$ (Table 3).

$$LH_3Fe^+ + H^+ \underset{k'_{-4}}{\overset{k'_4}{\rightleftharpoons}} LH_4Fe^{2+} \quad K'_4 = \frac{k'_4}{k'_{-4}} \quad (24)$$

$$LH_4Fe^{2+} + H^+ \underset{k'_{-5}}{\overset{k'_5,\text{rapid}}{\rightleftharpoons}} LH_5Fe^{3+} \quad K'_5 = \frac{k'_5}{k'_{-5}} \quad (25)$$

At the end of the reactions, the products obtained are LH_6^+ and Fe^{3+} in rapid equilibrium with $FeOH^{2+}$. It can therefore be assumed that, during the third step, the intermediate LH_5Fe^{3+} can dissociate according to two parallel paths:

$$LH_5Fe^{3+} + H^+ \underset{k'_{-6}}{\overset{k'_6}{\rightleftharpoons}} LH_6^+ + Fe^{3+} \quad K'_6 = \frac{k'_6}{k'_{-6}} \quad (26)$$

$$H^+ \updownarrow K_H$$

$$LH_5Fe^{3+} \underset{k'_{-7}}{\overset{k'_7}{\rightleftharpoons}} LH_6^+ + FeOH^{2+} \quad K'_7 = \frac{k'_7}{k'_{-7}} \quad (27)$$

From this model, the following rate expression, where $[LH_6^+]_e$ and $[Fe(III)]_e$ are the concentrations of the species at equilibrium, can be obtained:

$$k_{3,obs} = (k'_6[H^+] + k'_7) \times \frac{K'_4K'_5[H^+]^2}{(1 + K'_4K'_5[H^+]^2)} + \left(k'_{-6} + \frac{k'_{-7}K_H}{[H^+]}\right) \times ([LH_6^+]_e + [Fe(III)]_e) \quad (28)$$

In our conditions, $K'_4K'_5[H]^2 \gg 1$, and the fitting of our data by a non-least-squares regression shows that we cannot calculate k'_{-5} and k'_{-6}. The equation becomes linear with proton concentrations as we observed, $k_{3,obs} = k'_6[H^+] + k'_7$ with $k'_6 = b = 3.8(7) \times 10^{-3}\ M^{-1}\ s^{-1}$ and $k'_7 = c = 13.0(4) \times 10^{-3}\ s^{-1}$ (Table 3).

Considering now the absorptions A'_∞ and A''_∞ at the end of the second and the third steps, respectively (Figure 10), and using the previous proposed kinetic mechanisms, the expression of an apparent molar coefficient at 412 nm can be

Table 3. Kinetic, Thermodynamic, and Spectrophotometric Parameters Determined for the Acidic Dissociation of the Iron(III) Azotobactin δ Complexes[a]

elementary step	rate constant	thermodynamic constant	spectrophotometric data ϵ (M^{-1} cm^{-1}) at 412 nm
	First Step		
$LFe^{2-} + H^+ \rightleftarrows LHFe^-$		$K'_1 = 16000(5000)$ M^{-1}	$\epsilon_{LFe^{2-}} = 23\,000$
$LHFe^- + H^+ \rightleftarrows LH_2Fe$		$K'_2 = 1100(200)$ M^{-1}	$\epsilon_{LHFe^-} = 230\,000$
$LH_2Fe + H^+ \rightleftarrows LH_3Fe^+$		$K'_3 = 100(20)$ M^{-1}	$\epsilon_{LH_2Fe^+} = 23\,000$
	Second Step		
$LH_3Fe^+ + H^+ \underset{k'_{-4}}{\overset{k'_4}{\rightleftharpoons}} LH_4Fe^{2+}$	$k'_{4(abs)} = 4.63(4) \times 10^3$ M^{-1} s^{-1}		$\epsilon_{LH_3Fe^{2+}} = 15\,000$
	$k'_{4(fluo)} = 4.00(5) \times 10^3$ M^{-1} s^{-1}	$K'_4 \times K'_5 = 2.0(3) \times 10^3$ M^{-2}	
	$k'_{-4} \ll 5$ s^{-1}		
$LH_4Fe^{2+} + H^+ \underset{k'_{-5}}{\overset{k'_5}{\rightleftharpoons}} LH_5Fe^{3+}$	$k'_5 \gg k'_4$		$\epsilon_{LH_5Fe^{3+}} = 1500(400)$
	Third Step		
$LH_5Fe^{3+} + H^+ \underset{k'_{-6}}{\overset{k'_6}{\rightleftharpoons}} LH_6^+ + Fe^{3+}$	$k'_{6(abs)} = 3.8(7) \times 10^{-3}$ M^{-1} s^{-1}	$K'_6 = 1.48(7) \times 10^{-3}$	$\epsilon_{LH_6^+} = 730(30)$
	$k'_{6(fluo)} = 3.0(4) \times 10^{-3}$ M^{-1} s^{-1}		
	$k'_{-6} = 2.6(6)$ M^{-1} s^{-1}		$\epsilon_{Fe(III)} \sim 0$
$H^+ \updownarrow K_H$			
$LH_5Fe^{3+} \underset{k'_{-7}}{\overset{k'_7}{\rightleftharpoons}} LH_6^+ + FeOH^{2+}$	$k'_{7(abs)} = 13.0(4) \times 10^{-3}$ s^{-1}	$K'_7 = 2.2(1) \times 10^{-6}$ M	
	$k'_{7(fluo)} = 10.3(2) \times 10^{-3}$ s^{-1}		
	$k'_{-7} = 5.8(5) \times 10^3$ M^{-1} s^{-1}		

[a] Solvent: water; $I = 2.0$; $T = 25.0(2)$ °C.

calculated. For the second step, the LH_4Fe^{2+} concentration can be neglected, and the molar coefficients determined by our spectrophotometric studies, $\epsilon_{LFe^{2-}} = \epsilon_{LHFe^-} = \epsilon_{LH_2Fe} = 2.30 \times 10^4$ M^{-1} cm^{-1} and $\epsilon_{LH_3Fe^+} = 1.50 \times 10^4$ M^{-1} cm^{-1}, can be used. For the third step, it can be assumed that $\epsilon_{Fe(III)} \approx 0$ M^{-1} cm^{-1} and that $[Fe(III)]_e$ is independent of $[H^+]$ and equal to 2×10^{-5} M. Thus the following expressions can be obtained:

$$(A'_\infty)/(c_{tot} \times l)^{-1} = \{\epsilon_{LFe^{2-}} + \epsilon_{LHFe^-}K'_1[H^+] + \epsilon_{LH_2Fe}K'_1K'_2[H^+]^2 + \epsilon_{LH_3Fe} + K'_1K'_2K'_3[H^+]^3 + \epsilon_{LH_5Fe^{3+}}K'_1K'_2K'_3K'_4K'_5[H^+]^5\}/\{1 + K'_1[H^+] + K'_1K'_2[H^+]^2 + K'_1K'_2K'_3[H^+]^3 + K'_1K'_2K'_3K'_4K'_5[H^+]^5\}^{-1} \quad (29)$$

$$(A''_\infty)/(c_{tot} \times l)^{-1} = \{\epsilon_{LH_2Fe} + \epsilon_{LH_3Fe^+}K'_3[H^+] + \epsilon_{LH_5Fe^{3+}}K'_3K'_4K'_5[H^+]^3 + \epsilon_L K'_{H_6^{+3}}K'_4K'_5K'_6[H^+]^4/[Fe(III)]_e\}/\{1 + K'_3[H^+] + K'_3K'_4K'_5[H^+]^3 + K'_3K'_4K'_5K'_6[H^+]^4/[Fe(III)]_e\}^{-1} \quad (30)$$

From the adjustment of our data (Figure 10), the values $\epsilon_{LH_5Fe^{3+}} = 1500(400)$ M^{-1} cm^{-1}, $K'_4 \times K'_5 = 2000(300)$ M, $\epsilon_{LH_6^+} = 730(30)$ M^{-1} cm^{-1}, and $K'_6 = 1.48(7) \times 10^{-3}$ were obtained. Using the values of K'_6 and $K_H = 1.5 \times 10^{-3}$ determined by Milburn and Vosburgh,[59] K'_7 was calculated. From K'_6, K'_7, k'_6, and k'_7 determined previously, $k'_{-6} = 2.6(6)$ M^{-1} s^{-1} and $k_{-7} = 5800(500)$ M^{-1} s^{-1} could be easily deduced (Table 3).

Discussion

Equilibrium Studies. The deprotonation constant of the hydroxyl at position C-7 of the chromophore has the same value as for its homologue in pyoverdin PaA[27] ($pK_2 = 10.8$), 2.5 orders of magnitude higher than the pK value of 7-hydroxyquinoline[62,63] ($pK = 8.32$). The same difference is observed between the pK value of a phenol[64] ($pK = 9.98$) and the first deprotonation constant of a catechol[65] ($pK = 12.48$). The deprotonation constant of the other hydroxyl, at position C-6 of the chromophore moiety of azotobactin δ ($pK_4 = 6.3$), is 0.7 orders of magnitude lower than the pK value of the 6-hydroxyquinoline[62,63] ($pK = 7.02$), in agreement with the difference observed between the second protonation constants of the catechol group[65] ($pK = 9.45$) and the pK value of the phenol[64] ($pK = 9.98$). Since the protonation constant of the corresponding hydroxyl in the chromophore of pyoverdin PaA[27] ($pK = 5.6$) is 0.7 orders of magnitude lower, this difference has been assigned to the influence of a side chain bound to the chromophore in the case of pyoverdin PaA (Table 1).

The pK_3 value of the hydroxamate group of azotobactin δ ($pK_3 = 8.4$ (2) (Table 1) is very close to the third deprotonation constant of trihydroxamic acids or to the second deprotonation constant of dihydroxamic acids siderophores and is very similar to those determined for the hydroxamate groups of pyoverdin PaA in the same conditions (Table 4).[27]

The pK_5 value of 4.2(1) (Table 1) was assigned to the aspartic acid moiety of azotobactin δ, in agreement with literature values 3.94[66] and 3.7.[67] Unfortunately, it was impossible at our conditions to determine the pK_6 value of the carboxylic acid group of hydroxyaspartic acid (evaluated to 3.0 according to the literature)[51,52] and to measure the pK_1

(62) Schulman, S.; Fernando, Q. *Tetrahedron* **1968**, *24*, 1777−1783.
(63) Mason, S. F.; Philp, J.; Smith, B. E. *J. Chem. Soc. A* **1968**, 3051−3056.
(64) Tyson, C. A.; Martell, A. E. *J. Am. Chem. Soc.* **1968**, *90*, 3379−3386.
(65) Bordwell, F. G.; Cooper, G. D. *J. Am. Chem. Soc.* **1952**, *74*, 1058−1060.
(66) Ritsma, J. H.; Wiegers, G. A.; Jellinek, F. *Recl. Trav. Chim. Pays-Bas* **1965**, *84*, 1577−1585.
(67) Albert, A. *Biochem. J.* **1952**, *50*, 690−697.

Table 4. p*K* Values of Various Hydroxamic Compounds[a]

coordination site	siderophore	pK_1	pK_2	pK_3
3-hydroxamate	ferrichrome[60]	9.83	9.00	8.11
	ferrioxamine B[61]	9.70	9.03	8.39
	coprogen[57]	9.16	8.86	7.63
	TRENDROX[95]	10.30	9.33	8.58
coordination site	siderophore	pK_1	pK_2	
2-hydroxamate	rhodotorulic acid[96]	9.44	8.49	
	bisucaberin[97]	9.49	8.76	
	alcaligin[91]	9.42	8.61	
2-hydroxamate 1-hydroxyacid	aerobactin[58]	9.44	8.63	

[a] Solvent: water; $T = 25.0(1)$ °C.

Table 5. Reduction Potentals and Iron(III) and Iron(II) Thermodynamic Constants of Azotobactin δ and Various Natural Siderophores at p[H] = 7.40[a]

coordination site	siderophore	$E°$ (mV/NHE)	log $\beta_{LFe(III)}$	pFe(III)
3-catecholate	enterobactin[57,69,70]	−750	49	35.5
3-hydroxamate	ferrichrome[68]	−448	32.0	25.2
	ferrioxamine B[60]	−468	30.5	26.6
	coprogen[57]	−447	30.2	27.5
2-hydroxamate	rhodotorulic acid[96]	−415		21.9
	alcaligin[91]	−374		23.0
	bisucaberin[97]			22.5
2-hydroxamate 1-catecholate type	pyoverdin PaA[27]	−510	30.8	27.0
2-hydroxamate 1-hydroxyacid	aerobactin[58]	−336	22.5	23.3
1-catecholate 2-hydroxyacid	alterobactin B[97]	−448[b]	37.6[b]	27.8
1-hydroxamate 1-hydroxyacid 1-catechol type	azotobactin δ	−390	28.1	

[a] pM = −log[Fe]; [Fe] = 10^{-6} M; [L] = 10^{-5} M; p[H] = 7.40. [b] p[H] = 8.

value of the hydroxyl group of the hydroxyaspartic acid (pK > 11). Therefore, we used the L^{5-} notation for the fully deprotonated azotobactin δ. The values of all these constants are required to calculate the stability constant of the ferric complexes. We found four iron(III) complexes for azotobactin δ (Table 1) and compared them with other iron(III) siderophore complexes using the pFe(III) value calculated at p[H] = 7.40 for azotobactin δ (Table 5).

An α-hydroxyacid coordination site is a less powerful chelating group than a hydroxamic acid which is itself a less powerful chelating agent than a catechol function. The difference between azotobactin δ and aerobactin[58] occurs from the replacement of a hydroxamate group in aerobactin by a catechol coordination site in azotobactin δ. This explains why azotobactin δ forms stronger iron(III) complexes than aerobactin. Although ferric azotobactin δ complexes show stability constants closer to those of trishydroxamate siderophores (ferrichrome[68] or ferrioxamine B[60]) than to those of triscatecholate compounds (enterobactin[69,70]), these values are in agreement with the stability constants found at p[H] = 7 for various pseudobactins[8,9,18] and which vary from $10^{25.3}$ to $10^{26.1}$ M^{-1}. What are then the structures of ferric azotobactin δ complexes?

Table 6. Protonation Constants of Various α-Hydroxyacid Ligands and Their Iron(III) Complexes[a]

	protonation constant	
ligand	free ligand	ferric complex
azotobactin δ	log $K_6 = 3.0$	log $K_{LH_2Fe} = 3.0$ log $K_{LH_3Fe^+} = 2.0$
aerobactin[58]	log $K_1 = 4.31$ log $K_2 = 3.48$ log $K_3 = 3.11$	log $K_{LFe^{2-}} = 4.58$ log $K_{LHFe^-} = 3.62$ log $K_{LH_2Fe} = 3.02$ log $K_{LH_3Fe^+} = 2.04$
rhizoferrin[77]	log $K_1 = 4.21(4)$ log $K_2 = 3.05(6)$ log $K_3 = 2.86(7)$	log $K_{LHFe^-} = 5.5(4)$ log $K_{LH_2Fe} = 4.3(3)$ log $K_{LH_3Fe^+} = 1.8(3)$
lactobionic acid[71]	log $K = 3.53$	log $K_{LH_{-1}Fe^+} = 3.89$ log $K_{LFe^{2+}} = 2.03$
citric acid[72]	log $K_1 = 5.7$ log $K_2 = 4.36$ log $K_3 = 2.81$	log $K_{LFe} = 2.6$ log $K_{LHFe^+} = 1.2$

[a] Solvent: water; $I = 0.1$; $T = 25.0$ °C.

Considering the protonation constants of the following different species:

$$LFe^{2-} + H^+ \rightleftarrows LHFe^- \quad \log K'_1 = 4.2 \qquad (31)$$

$$LHFe^- + H^+ \rightleftarrows LH_2Fe \quad \log K'_2 = 3.0 \qquad (32)$$

$$LH_2Fe + H^+ \rightleftarrows LH_3Fe^+ \quad \log K'_3 = 2.0 \qquad (33)$$

In agreement with the pK value of free aspartic acid (pK = 3.7[63] or 3.94[62]), K'_1 can easily be assigned to the protonation of the aspartic acid moiety located on the peptidic chain of azotobactin δ, which is not involved in iron(III) coordination. The assignment of K'_2 and K'_3 is more difficult, these values corresponding to those of ferric protonated complexes of a α-hydroxycarboxylic acid[58,71,72] (Table 6).

Actually, if K'_2 is assigned to the protonation of the carboxylic group, it means that this function is not involved in the iron(III) coordination, because this value (3.0) is similar to the value of a free carboxylic acid[58,73−75] (Table 6). However, since for azotobactin δ as for aerobactin, the central carboxylate group is an iron(III) binding site, we suggest that K'_2 and K'_3 are the protonation constants of, respectively, the hydroxyl and the carboxyl groups. ^{13}C NMR and ^1H NMR measurements and crystal structures of citric acid transition metal complexes show the protonated hydroxyl function coordinated to the metal. This is corroborated by kinetic studies performed by Mentasti[73] on the formation of the ferric complexes of α-hydroxycarboxylic acids showing that the last step corresponds to the labilization of the hydroxyl function. Thus, using the reverse mechanism, this group is the first to be protonated confirming our hypothesis.

(68) Wawrousek, E. F.; McArdle, J. V. *J. Inorg. Biochem.* **1982**, *17*, 169−183.
(69) Harris, W. R.; Carrano, C. J.; Cooper, S. R.; Sofen, S. R.; Avdeef, A. E.; McArdle, J. V.; Raymond, K. N. *J. Am. Chem. Soc.* **1979**, *101*, 6097−6104.
(70) Loomis, L. D.; Raymond, K. N. *Inorg. Chem.* **1991**, *30*, 906−911.
(71) Field, T. B.; McCourt, J. L.; McBryde, W. A. E. *Can. J. Chem.* **1974**, *52*, 3119-3124.
(72) Escandar, G. M.; Olivieri, A. C.; Gonzales-Sierra, M.; Sala, L. F. *J. Chem. Soc.*, Dalton Trans. **1994**, 1189-1192.
(73) Mentasti, E. *Inorg. Chem.* **1979**, *18*, 1512−1515.
(74) Crumbliss, A. L. In *Handbook of Microbial Iron Chelates*; Winkelmann, G., Ed; CRC Press: Boca Raton, FL, 1991; pp 177−232.
(75) Sen Gupta, K. K.; Chatterjee, A. K. *J. Inorg. Nucl. Chem.* **1976**, *38*, 875−876.

The protonation of azotobactin δ induces a shift of the absorption maxima toward shorter wavelengths together with a decrease of absorption, in agreement with the spectrophotometric results obtained for 6-, 7-hydroxyquinoline[62,63] and for various pseudobactins[6,9] and pyoverdins.[8,14,18,27] Although the electronic spectra of the monoprotonated chromophore of azotobactin δ ($\lambda_{max} = 408$ nm, $\epsilon_{max} = 2.62 \times 10^4$ M^{-1} cm^{-1}) and of pyoverdin PaA[27] ($\lambda_{max} = 402$ nm, $\epsilon_{max} = 2.82 \times 10^4$ M^{-1} cm^{-1}) are similar, the diprotonated form shows different absorption maxima and molar extinction coefficients. The presence of a side chain bound at position C-3 of the chromophore of pyoverdin PaA seems to play an important role during the protonation on the absorption ($\lambda_{max} = 364$ nm ($\epsilon_{max} = 1.70 \times 10^4$ M^{-1} cm^{-1} for pyoverdin PaA[27] and $\lambda_{max} = 378$ nm ($\epsilon_{max} = 2.43 \times 10^4$ M^{-1} cm^{-1}) for azotobactin δ). The electronic spectra of the hexacoordinated ferric complexes (LFe^{2-}, $LHFe^{-}$) of ferric azotobactin δ (Figure 3) show a maximum at 412 nm ($\epsilon_{max} = 2.30 \times 10^4$ M^{-1} cm^{-1}) and two shoulders, one at 440 nm ($\epsilon \sim 1.40 \times 10^4$ M^{-1} cm^{-1}) corresponding to the charge-transfer band of hydroxamate to Fe(III) and the other at 540 nm ($\epsilon \sim 2.6 \times 10^3$ M^{-1} cm^{-1}) corresponding to the charge-transfer band of the catechol to iron(III).[29,74] Similar absorptions were observed for the ferric complexes of pseudobactin 589 A[9] ($\lambda_{max} = 398$ nm, $\epsilon = 1.95 \times 10^4$ M^{-1} cm^{-1}, shoulder at 450 nm, $\epsilon = 5.0 \times 10^4$ M^{-1} cm^{-1}), pseudobactin[6] ($\lambda_{max} = 400$ nm, $\epsilon = 2.10 \times 10^4$ M^{-1} cm^{-1}, shoulders at 460 nm, $\epsilon = 6.0 \times 10^3$ M^{-1} cm^{-1} and 540 nm, $\epsilon = 3.0 \times 10^3$ M^{-1} cm^{-1}), and pyoverdin G4R[14] ($\lambda_{max} = 400$ nm, $\epsilon = 1.95 \times 10^4$ M^{-1} cm^{-1}, shoulders at 460 nm, $\epsilon = 6.0 \times 10^3$ M^{-1} cm^{-1} and 540 nm, $\epsilon = 3.0 \times 10^3$ M^{-1} cm^{-1}), three siderophores with the same iron(III) coordination sites as azotobactin δ. The formation of the species LH_3Fe^{+} induces an important change in the UV−vis spectral properties: the maximum shifts to 390 nm ($\epsilon \sim 2.15 \times 10^4$ M^{-1} cm^{-1}), and the hydroxamate Fe(III) and catechol Fe(III) charge-transfer bands[74] shift, respectively, to 490 nm ($\epsilon = 5.5 \times 10^4$ M^{-1} cm^{-1}) and to 550 nm ($\epsilon = 3.5 \times 10^4$ M^{-1} cm^{-1}), suggesting that iron(III) is tetracoordinated to the ligand after dissociation of the α-hydroxycarboxylic group. No absorbtivity differences due to the carboxylic function could be observed[75−77] (360 nm $< \lambda_{max} <$ 375 nm and 1.9×10^3 M^{-1} $cm^{-1} < \epsilon < 3.0 \times 10^3$ M^{-1} cm^{-1}) since the absorptions relative to this function are hidden by the chromophore absorption ($\lambda_{max} = 390$ nm, $\epsilon = 2.15 \times 10^4$ M^{-1} cm^{-1}).

The redox potential of ferric azotobactin δ complexes at − 390 mV/NHE is much less negative than the value reported for triscatecholates complexes[69,70] ($E° \sim -750$ mV/NHE) (Table 5).

Ferrioxamine B, a trishydroxamate siderophore[68] ($E° \sim -468$ mV/NHE), or aerobactin,[57] a mixed siderophore with two hydroxamates and one α-hydroxyacid binding site ($E° \sim -336$ mV/NHE), shows a similar behavior. Thus, the redox potential of ferric azotobactin δ complexes is accessible to physiological reductants which can easily reduce the azotobactin−Fe(III) complex into the easily dissociable azotobactin−Fe(II) complex, suggesting strongly that an iron(II) release mechanism could be involved for iron deposition into the cell.

Table 7. Reactivity of $Fe(OH)^{2+}$ and $Fe_2(OH)_2^{4+}$ with Azotobactin δ and Various Hydroxamate, Catecholate, and Hydroxyacid Compounds

ligand	k_f ($Fe(OH)^{2+}$) × 10^{-3} (M^{-1} s^{-1})	k_f ($Fe_2(OH)_2^{4+}$) × 10^{-3} (M^{-1} s^{-1})
azotobactin δ LH_6^{+}	5.9 (4)	
LH_5	21 (3)	610 (30)
monohydroxamic acid[87,88]	[0.46−1.2]	
acetohydroxamic acid[98]	5.7 (9)	8.2 (1.3)
desferriferrioxamine B[83]	3.6 (2)	
pyoverdin PaA[27]	7.7	50
catechol[99]	3.1 (2)	
substituted catecholates[100]	[1.7−2.9]	
tiron[101]	3.1	11
α-hydroxycarboxylic acids[73,101−103]	[2.3−26]	

Circular Dichroism. X-ray diffraction is the unique method to determine unambiguously the absolute configuration of a given compound. In the absence of crystals, as is the case for azotobactin δ, the chirality of a given complex around the central ion can be deduced by comparison of its CD spectrum with the spectrum of an analogue whose configuration is well established and taken as a reference. van der Helm et al.[54] have shown that ferrichrome presents the same CD spectrum in solution and in crystalline form (Λ cis). An empirical law for the determination of the absolute configuration of Cr(III) complexes was devised using the sign of the Cotton effect for the absorption band in the visible. The comparison between the siderophore-Cr(III) and -Fe(III) complexes shows that this empirical law can be used for ferric compounds: If the Cotton effect in the charge-transfer band of the CD spectrum of catecholate-Fe(III) or hydroxamate-Fe(III) complexes is positive, then these complexes present a predominant Λ configuration in solution. On the contrary, a negative Cotton effect indicates a Δ configuration. Using this empirical law, it can be deduced that azotobactin δ ferric complexes have a predominant Λ absolute configuration in solution.

Formation Kinetics. From our results, it can be concluded that the formation of the ferric complexes of azotobactin δ occurs according to two parallel paths giving rise to the LH_5Fe^{3+} species followed by rapid coordination of the other bidentate sites. Three iron(III) species are involved in this reaction, Fe^{3+}, $Fe(OH)^{2+}$, and $Fe_2(OH)_2^{4+}$, and two forms of azotobactin δ, LH_5 and LH_6^{+}, can react. The results concerning the formation of iron(III) complex with different ligands are presented in Table 7.

The rate constant of the formation of azotobactin δ ferric complex with $Fe(OH)^{2+}$ is in agreement with literature values, and the corresponding reaction is consistent with the I_d dissociative mechanism proposed for these ferric species[78] in agreement with classical Eigen−Wilkins[79] metal complex formation, with a fast formation step of an outer-sphere complex (K_{os}) followed by a metal desolvation rate-limiting step (k_{ex}) following the Fuoss equation:

$$k_{Fe(OH)^{2+}} = K_{os} k_{ex} \quad (34)$$

(76) Timberlake, C. F. *J. Chem. Soc.* **1964**, 5078−5085.
(77) Carrano, C. J.; Drechsel, H.; Kaiser, D.; Jung, G.; Matzanke, B.; Winkelmann, G.; Rochel, N.; Albrecht-Gary, A. M. *Inorg. Chem.* **1996**, *35*, 6429−6436.

The value of K_{os} can be evaluated using the water exchange method determined by NMR measurements[80] (1.2×10^5 s^{-1}) giving rise for the two reacting forms of azotobactin δ to the following expressions:

$$K_{os}(LH_6^+, Fe(OH)^{2+}) = 5.9 \times 10^3/1.2 \times 10^5 = 0.05\ M^{-1}$$

$$K_{os}(LH_5, Fe(OH)^{2+}) = 21 \times 10^3/1.2 \times 10^5 = 0.17\ M^{-1}$$

The K_{os} value calculated for the LH_6^+ species of azotobactin δ (0.05 M^{-1}) is very similar to the value calculated for ferrioxamine B (0.03 M^{-1}).[81] The LH_5 form of azotobactin δ is more reactive certainly due to a more stable outer-sphere complex.

Dissociation Kinetics. From Table 3 it is clear that absorption and fluorescence measurements give the same results (Table 3) according to the following mechanism for the dissociation of azotobactin δ- ferric complexes in acidic media:

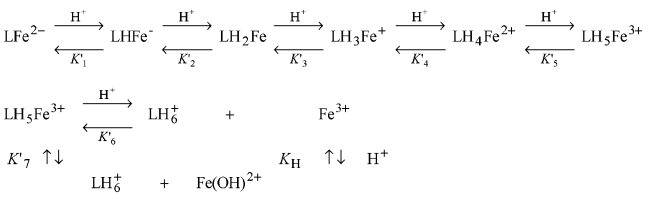

Starting with the LFe^{2-} species, the first kinetic intermediate observed and characterized by its electronic spectrum is the LH_3Fe^+ complex. However, the rate of formation of this complex is too high to be measured in our conditions, and an unusual mechanism with the dissociation of the central coordination site is observed, contrary to ferrioxamine B[82,83] and pyoverdin PaA[27] for which an unfolding of the ligand around the ferric cation was observed.

The second step, with two protons involved leading to the formation of LH_4Fe^{2+}, is rate-limiting and is followed by the rapid formation of the LH_5Fe^{3+} species. The variations measured between the electronic spectra of LH_3Fe^+ and LH_5Fe^{3+} (Figure 9) show that these protonations are located on the chromophore. Such behavior, i.e. one step and two protons involved, was already observed in the formation of TRIMCAMS (an enterobactin analogue) ferric complex and assigned to the simultaneous protonation of the two hydroxyl groups of the dihydroxybenzamide moiety.[84] In the case of azotobactin δ, the same mechanism with successive protonation of the catechol moiety was observed, supported by the fact that it is not possible to assign the rate constant $k'_4 \sim 4 \times 10^3$ M^{-1} s^{-1} to the hydroxamate dissociation which is much slower than the catecholate.[27,82,83,85] The comparison with pyoverdin PaA shows that this value corresponds to the dissociation of the second proton of the chromophore of pyoverdin PaA,[27] the first one being faster. Therefore, the protonation of the quinoleine group of azotobactin δ must occur in the opposite order compared to pyoverdin PaA for which the protonation of the second hydroxyl group is the rate-limiting step. The LH_5Fe^{3+} complexes correspond to the protonation of the α-hydroxycarboxylic and the catechol group; however, a high fluorescence inhibition is still observed. This may be due either to electron transfer from ligand to metal or to spin−orbital coupling with enhancement of intersystem transitions which help to reach the ground state via the triplet state. Spin−orbital coupling inhibition needs an overlap of the iron d-orbitals with the ligand π-orbitals, and electron-transfer inhibition depends on the distance from the two orbitals. This latter should be less than 10 Å to have efficient inhibition.[86] In both cases, iron should be close to the chromophore, and therefore, one hydroxyl group is in the first or in the second iron(III) coordination sphere. This shows that the ligand keeps a closed conformation due certainly to hydrogen bonds which may stabilize the complex as observed for ferrichrome analogues.[84] This mechanism differs from those reported for pyoverdin PaA[27] and ferrioxamine B[82,83] where the ligands unfold from the iron(III) coordination cage.

The third step actually concerns the dissociation of the monohydroxamic group, the last iron(III) coordination site. This is in agreement with the variation of the electronic spectra which corresponds to the disappearance of the charge-transfer band centered at about 510 nm which is characteristic of monohydroxamic ferric complexes[87,88] (Figure 9b). An intense fluorescence emission is observed, showing that iron(III) leaves the coordination cage and is no longer close to the chromophore. Our kinetic data are in agreement with literature data on iron(III) monohydroxamate complexes[82,83,87,89,90] via two parallel paths leading to the liberation of the $Fe(H_2O)_6^{3+}$ species (proton dependent path) and

(78) Grant, M.; Jordan, R. B. *Inorg. Chem.* **1981**, *20*, 55-60.
(79) Eigen, M.; Wilkins, R. G. *Adv. Chem. Ser.* **1965**, *49*, 55−67.
(80) Swaddle, T. W.; Merbach, A. E. *Inorg. Chem.* **1981**, *20*, 4212−4216.
(81) Batinic-Haberle, I.; Birus, M.; Pribanic, M. *Inorg. Chem.* **1991**, *30*, 4882−4887.
(82) Monzyk, B.; Crumbliss, A. L. *J. Am. Chem. Soc.* **1982**, *104*, 4921−4929.
(83) Birus, A.; Bradic, Z.; Krznaric, G.; Kujundzic, N.; Pribanic, M.; Wilkins, P. C.; Wilkins, R. G. *Inorg. Chem.* **1987**, *26*, 1000−1005.
(84) Harris, W. R.; Raymond, K. N.; Weitl, F. L. *J. Am. Chem. Soc.* 1981, *103*, 2667−2675.
(85) Zhang, Z.; Jordan, R. B. *Inorg. Chem.* **1996**, *35*, 1571−1576.
(86) Eftink, M. R. *Topics in Fluorescence Spectroscopy*; Principles, J. R., Lakowicz, J. R., Eds.; Plenum Press: New York, 1991; Vol. 2, p 53.
(87) Monzyk, B.; Crumbliss, A. L. *J. Am. Chem. Soc.* **1979**, *101*, 6203−6213.
(88) Brink, C. P.; Crumbliss, A. L. *Inorg. Chem.* **1984**, *23*, 4708−4718.
(89) Caudle, M. T.; Cogswell, L. P.; Crumbliss, A. L. *Inorg. Chem.* **1994**, *33*, 4759−4773.
(90) Caudle, M. T.; Crumbliss, A. L. *Inorg. Chem.* **1994**, *33*, 4077−4085.
(91) Hou, Z.; Raymond, K. N.; O'Sullivan, B.; Esker, T. W. *Inorg. Chem.* **1998**, *37*, 6630−6637.
(92) Tor, Y.; Libman, J.; Shanzer, A.; Felder, C. E.; Lifson, S. *J. Am. Chem. Soc.* **1992**, *114*, 6661−6671.
(93) Akiyama, M.; Ikeda, T. *Chem. Lett.* **1995**, 849−850.
(94) Bergeron, R.; Weimar, W. R. *J. Bacteriol.* **1990**, *172*, 2650−2657.
(95) Ng, C. Y.; Rodgers, S. J.; Raymond, K. N. *Inorg. Chem.* **1989**, *28*, 2062−2066.
(96) Carrano, C. J.; Cooper, S. R.; Raymond, K. N. *J. Am. Chem. Soc.* **1979**, *101*, 599−604.
(97) Lewis, B. L.; Holt, P. D.; Taylor, S. W.; Wilhem, S. W.; Trick, C. G.; Butler, A.; Luther, G. W., III. *Mar. Chem.* **1995**, 179−188.
(98) Birus, M.; Kujundzic, N.; Pribanic, M. *Inorg. Chim. Acta* **1980**, *55*, 65−69.
(99) Mentasti, E.; Pelizzetti, E. *J. Chem. Soc., Dalton Trans.* **1973**, 2605−2608.
(100) Mentasti, E.; Pelizzetti, E.; Saini, G. *J. Inorg. Nucl. Chem.* **1976**, *38*, 785−788.
(101) Xu, J.; Jordan, R. B. *Inorg. Chem.* **1988**, *27*, 1502−1507.
(102) Gilmour, A. D.; McAuley, A. *J. Chem. Soc. A* **1969**, 2345−2348.
(103) Miftahova, A.; Dozsa, L.; Beck, M. T. *Acta Chim. Budapest* **1977**, *92*, 379−386.

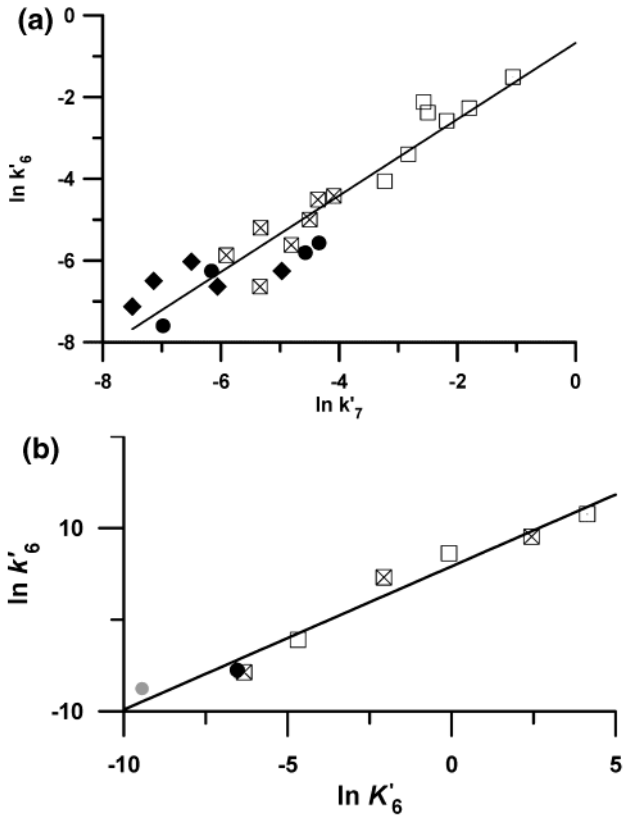

Figure 11. (a) Variation of ln k'_6 as a function of ln k'_7 for the bidentate ferric complex dissociation. Monohydroxamate complexes: box = $Fe(H_2O)_4(R_CC(O)N(O)H)^{2+}$, box with × = $Fe(H_2O)_4(R_CC(O)N(O)R_N)^{2+}$, diamond = bidentate-dihydroxamate complexes, gray filled circle = bidentate-trishydroxamate complexes, black filled circle = azotobactin δ monohydroxamate. (b) ln k'_6 variation as a function of ln K'_5 for dissociation reaction of mono-, di- and tris-hydroxamate iron(III) complexes. Acetohydroxamate anion (box): 1, $Fe(AHA)_3$; 2, $Fe(AHA)_2^+$; 3, $Fe(AHA)^{2+}$. *N*-Methylacetohydroxamate anion (box with ×): 4, $Fe(NMHA)_3$; 5, $Fe(NMHA)_2^+$; 6, $Fe(NMHA)^{2+}$. Bidentate form of ferrioxamine B (gray filled circle): 7, FeH_3DFB^{3+}. Monohydroxamate form of azotobactin δ (black filled circle): 8, LH_4Fe^{2+}. Solvent: water; $I = 2.0$; $T = 25$ °C.

the $Fe(H_2O)_5OH^{2+}$ (proton independent path). The rate constant k'_6 and the stability constant K'_6 of the dissociation of the monohydroxamate site of azotobactin δ are of the same order of magnitude as those of *N*-methyl substituted monohydroxamic acids.[87,88,90] The rate constant k'_7 corresponding to the proton independent path is between 2 and 10 orders of magnitude higher than those of tri- or dihydroxamate complexes dissociation sites but remains in the same range as those of N-methyl or N-phenyl substituted monohydroxamate complexes.[87,88,90]

Figure 11a shows the linear relationship between proton-mediated dissociation and the equation mechanism whose transition states differ only by the presence of a proton. The deviation from unity in Figure 11a (slope ≅ 1.5) could be due to a small role played by the ligand in a so-called "late" transition state where the metal−ligand bonds are not completely broken. Since the data in Figure 11a show the same correlation for various bidentate hydroxamic acids and ferrioxamine B, the final dissociation of the hydroxamate group appears to be independent of the chemical structure of the ligand (see refs 89 and 90 and references therein).

Figure 11b confirms these conclusions for the proton-mediated step and suggests in agreement with literature data (see refs 89 and 90 and references therein) that the final dissociation of the monohydroxamate group of azotobactin δ is similar to those of iron(III) monohydroxamate complexes, with a rapid cleavage of the Fe−O(N) bond followed by the rate-limiting cleavage of the Fe−O(C) bond. Close values of the dissociation rates of the hydroxamate site of azotobactin δ and *N*-methylacetohydroxamate (often used as a model for siderophores) were observed as well (Figure 11). The possibility of an intramolecular H^+ transfer from the carboxylic acid ($\log K'_6 = 3.0$) to the hydroxamate group was also considered. This proton independent path gives rise to LH_5 and Fe^{3+}. Fitting this mechanism to our data gives a reverse reaction rate constant of 8000 M^{-1} s^{-1} which is 3 orders of magnitude higher than those obtained for the formation of iron(III) complexes with Fe^{3+} cation, ruling out this possibility. The rate constant k'_{-7} calculated from the dissociation kinetics measurements ($k'_{-7} = 5800(500)$ M^{-1} s^{-1}) is similar to that obtained during the kinetics of formation of azotobactin δ LH_6^+ species and $Fe(OH)^{2+}$ ($k_3 = 5900(400)$ M^{-1} s^{-1}) confirming our mechanism.

The reverse rate constant k_{-6} could not be determined by our kinetic analysis. However, it should be in agreement with literature values (1−6 M^{-1} s^{-1})[79,87,88] for the coordination site of hydroxy acids.

From our kinetic data, the stability constant *K* of the ferric complexes corresponding to the following equilibrium can also be determined:

$$LH_6^+ + Fe^{3+} \rightleftarrows LFe^{2-} + 6H^+ \quad K = \frac{[LFe^{2-}][H^+]^6}{[LH_6^+][Fe^{3+}]} \qquad (35)$$

Since $K = (K'_1K'_2K'_3K'_4K'_5K'_6)^{-1}$, using $K'_1K'_2K'_3$ values determined from potentiometric and spectrophotometric data, and $K'_4K'_5$ and K'_6 from kinetics measurements, the value of $K = 1.9 \times 10^{-10}$ M^{-5} can easily be calculated. This value is very similar to the value $K = 1.3 \times 10^{-9}$ M^{-5} determined from thermodynamic studies. Figure 12 summarizes our mechanism.

Conclusion

With three different binding sites, a catecholate group (on the chromophore), a hydroxamate function (at the end of the peptidic chain), and a hydroxyacid (in the middle of the peptidic chain) the bacterial siderophore, azotobactin δ, forms octahedral ferric complexes in a predominant Λ configuration in solution. The pFe(III) values, calculated for ferric azotobactin δ, are very similar to the corresponding data reported for trishydroxamate siderophores. The redox potential of the azotobactin δ iron complexes is consistent with a reductive

(104) Abbreviations used in this paper include the following. The chromophore is referred as Chr. For the peptide chain, the following shorthand is used: Asp, (L)-aspartic acid; HOAsp, (D)-β−*threo*-hydroxyaspartic acid; Gly, glycine; (D)-Ser, (D)-serine; (L)-Ser, (L)-serine; (L)-Hse, (L)-homoserine; (L)-Hse lactone, (L)-homoserine lactone; (D)-Cit, (D)-citrulline HOOrn, (D)-N^δ-Ac, N^δ-HOOrn, (D)-N^δ-acetyl, N^δ-hydroxyornithine. CD refers to circular dichroism. AHA is the abbreviation for acetohydroxamate anion, NMHA is for *N*-methylacetohydroxamate anion, and DFB is for desferriferrioxamine B.

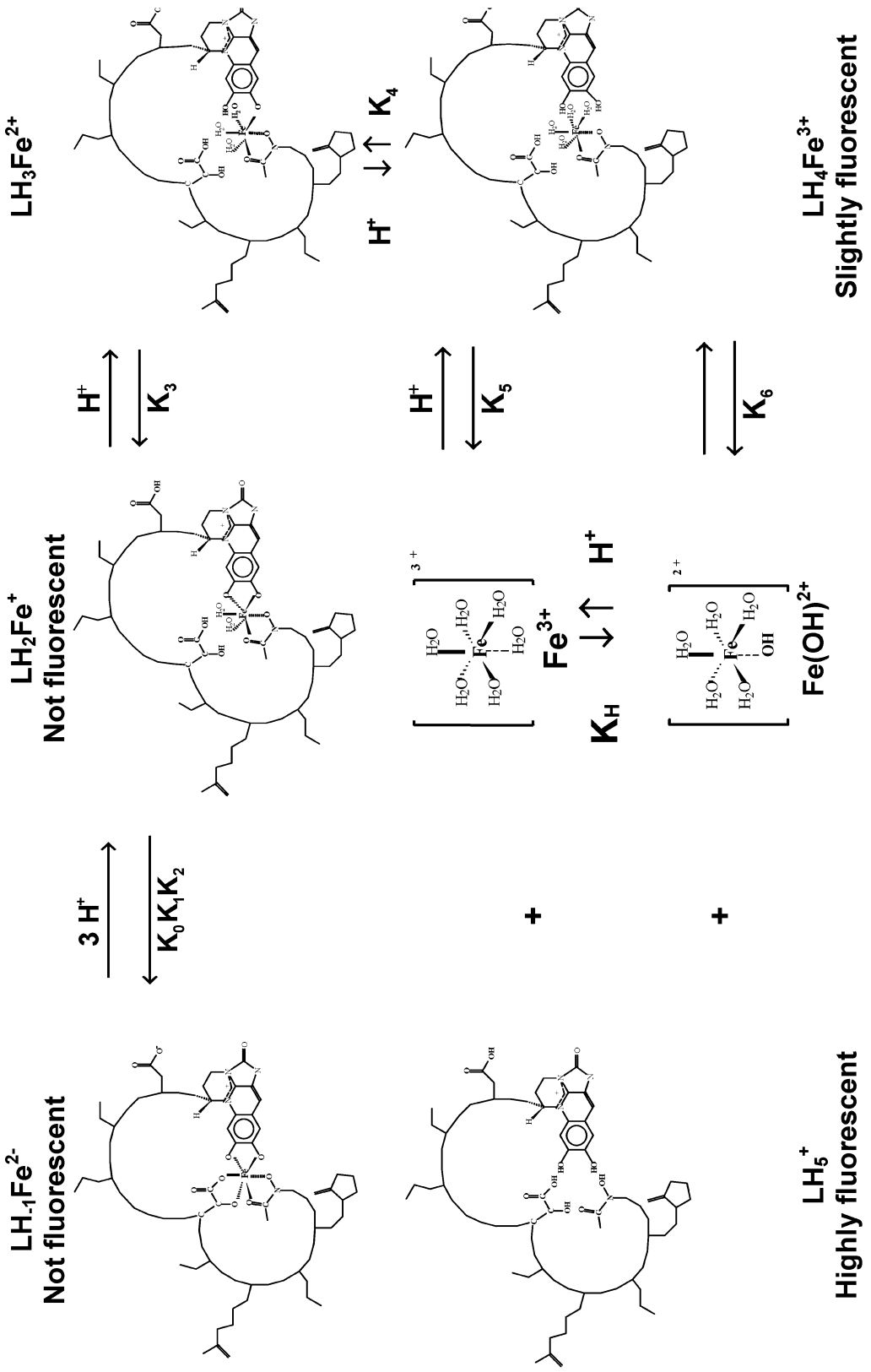

Figure 12. Proton-mediated dissociation mechanism of ferric azotobactin δ.

step by physiological reductants for the iron release in its reduced form Fe(II).

The coordination process of $Fe(OH)^{2+}$ by azotobactin δ shows an Eigen−Wilkins mechanism, with a single rate-limiting step related to the coordination of the terminal hydroxamate function. The dissociation of the azotobactin δ iron(III) complex occurs in acidic media with a very efficient step by step mechanism. The proton-mediated dissociation process showed a fast release of the α-hydroxycarboxylic group followed by a slower dissociation of the catechol-like unit, the final step being related to the hydroxamate end.

Formation and dissociation kinetics of the azotobactin δ ferric complex point out that both ends of this long siderophore chain get coordinated to Fe(III) before the middle. The most striking result provided by fluorescence measurements is the lasting quenching of the fluorophore in the course of the protonation of the azotobactin δ ferric complex. Despite the release of the hydroxyacid and of the catechol, the fluorescence remains indeed quenched, when iron(III) is bound only to the hydroxamic acid, suggesting a folded conformation at this stage.

Acknowledgment. The authors wish to thank Mr. Nicolas Humbert for the ball-and-cylinder representation of azotobactin δ ferric complex, and the Centre National de la Recherche Scientifique and the Ministère de la Recherche et de la Technologie for financial support (ACC-SV5, Physique et Chimie du Vivant 1997 and ATP Microbiologie 1998).

Supporting Information Available: Additional figure and table. This material is available free of charge via the Internet at http://pubs.acs.org.

IC034862N